Published in final edited form as:

J Org Chem. 2022 June 17; 87(12): 7934–7944. doi:10.1021/acs.joc.2c00587.

Chiral Recognition of Hydantoin Derivatives Enabled by Tetraaza Macrocyclic Chiral Solvating Agents Using ^{1}H NMR Spectroscopy

Jie Wen,
College of Chemistry, Beijing Normal University, Beijing 100875, P. R. China

Lei Feng,
College of Chemistry, Beijing Normal University, Beijing 100875, P. R. China

Hongmei Zhao,
State Key Laboratory of Information Photonics and Communications, School of Science, Beijing University of Posts and Telecommunications, Beijing 100876, P. R. China

Li Zheng,
College of Chemistry, Beijing Normal University, Beijing 100875, P. R. China

Pericles Stavropoulos,
Department of Chemistry, Missouri University of Science and Technology, Rolla, Missouri 65409, United States

Lin Ai,
College of Chemistry, Beijing Normal University, Beijing 100875, P. R. China

Jiaxin Zhang
College of Chemistry, Beijing Normal University, Beijing 100875, P. R. China

Abstract

Enantiomers of a series of hydantoin derivatives were prepared from D- and L-amino acids with *p*-tolyl isocyanate and 3,5-bis(trifluoromethyl)phenyl isocyanate as guests for chiral recognition by ^{1}H NMR spectroscopy. Meanwhile, several tetraaza macrocyclic compounds were synthesized as chiral solvating agents from D-phenylalanine and (1*S*,2*S*)-(+)-1,2-diaminocyclohexane. An uncommon enantiomeric discrimination has been successfully established for hydantoin derivatives, representatives of five-membered N,N-heterocycles, in the presence of tetraaza macrocyclic chiral solvating agents (TAMCSAs) **1a–1c** by means of ^{1}H NMR spectroscopy. Several unprecedented nonequivalent chemical shifts (un to 1.309 ppm) were observed in the

Corresponding Authors: **Lin Ai** – *College of Chemistry, Beijing Normal University, Beijing 100875, P. R. China;* linai@bnu.edu.cn; **Jiaxin Zhang** – *College of Chemistry, Beijing Normal University, Beijing 100875, P. R. China;* zhangjiaxin@bnu.edu.cn.

Supporting Information

The Supporting Information is available free of charge at https://pubs.acs.org/doi/10.1021/acs.joc.2c00587.

NMR and HRMS spectra of TAMCSAs **1a–c**, chiral compounds **2a–2c**, and enantiomers of hydantoin derivatives (G**1–14**) for all new compounds; ^{1}H NMR spectra of chiral recognition of (±)-G**1–14**; optimization of chiral discriminating conditions; and DFT and related data (PDF)

Complete contact information is available at: https://pubs.acs.org/10.1021/acs.joc.2c00587

The authors declare no competing financial interest.

split ^{1}H NMR spectra. To evaluate practical applications in the determination of enantiomeric excess (ee), the ee values of samples with different optical purities (up to 95% ee) were accurately calculated by the integration of relevant proton peaks. To better understand the chiral discriminating behavior, Job plots of (±)-G**1** with TAMCSA **1a** were investigated. Furthermore, in order to further explore any underlying intermolecular hydrogen bonding interactions, theoretical calculations of the enantiomers of (*S*)-G**1** and (*R*)-G**1** with TAMCSA **1a** were performed by means of the hybrid density functional theory (B3LYP/6-31G*) of the Gaussian 16 program.

Graphical Abstract

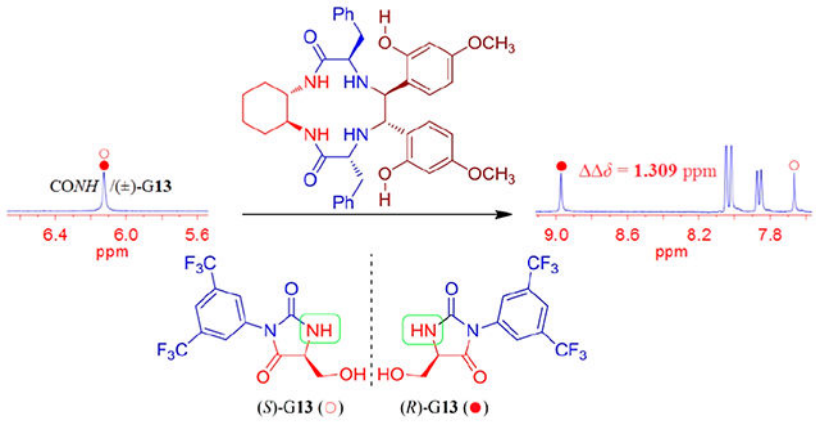

INTRODUCTION

Chiral recognition is one of the most significant topics in a variety of research fields, such as catalytic asymmetric chemistry and chiral pharmaceuticals, biology, and life science.[1] Among them, assignment of the absolute configuration of chiral molecules and determination of enantiomeric excess (ee) of chiral compounds are indispensable elements of structural characterization and practical applications because different enantiomers possess different optical properties, biological activities, and pharmacological (even toxic) effects.[2] For this purpose, a variety of techniques and methods, such as high-performance liquid chromatography,[3] X-ray crystallography,[4] circular dichroism (CD),[5] vibrational CD,[6] nuclear magnetic resonance (NMR),[7] UV–vis, and fluorescence spectroscopy,[8] have been developed and utilized separately or in tandem. Among these available techniques, the ^{1}H NMR technique has several obvious advantages, associated with simple and fast measurement, accurate and convenient application, and employment of a low amount of samples, as well as the availability of a ubiquitous NMR apparatus in nearly all chemical laboratories.[9] Thus, the NMR technique has widely emerged as the commonly applied tool for the determination of absolute configuration and quantitative analysis of ee of chiral substrates.[10] In the course of research on chiral recognition, on the one hand, effective chiral auxiliaries play a key role in chiral discriminating behavior between hosts and guests by NMR spectroscopy because the differentiation of chiral substrates relies on the generation of a pair of diastereomeric adducts by means of covalent bond formation or noncovalent interactions with chiral auxiliaries (chiral derivatizing agents and chiral solvating agents).[11] To explore chiral auxiliaries with sufficient sensitivity and high chiral

discriminating performance, various chiral auxiliaries have been designed, synthesized, and screened through the continuous efforts of chemists.[12] On the other hand, chiral recognition of a variety of chiral substrates should be explored and investigated to further deepen and promote the development of chiral recognition and its related applications by ^{1}H NMR spectroscopy. In the past decades, chiral recognition of acyclic compounds, such as chiral amines,[13] amino alcohols,[14] alcohols,[15] amino acids or their derivatives,[16] carboxylic acids,[17] and esters,[18] has been frequently reported by means of ^{1}H NMR spectroscopy. In recent years, we have also reported some studies on chiral recognition of α-hydroxy acids, α-amino acid derivatives, dipeptide derivatives with two chiral centers, and tripeptide derivatives with three stereogenic centers as acyclic substrates in the presence of a series of tetraaza macrocyclic chiral solvating agents (TAMCSAs) by means of ^{1}H NMR spectroscopy. Based on these results, these TAMCSAs have been successfully established as a family of versatile and highly effective chiral solvating agents vis-à-vis the aforementioned acyclic compounds.[19] Nevertheless, recognition of chiral cyclic substrates has rarely been investigated by ^{1}H NMR spectroscopy.[20] This is surprising, given the fact that enantiomerically pure cyclic products, including several chiral hydantoin derivatives, have been used to treat many human diseases, due to their powerful physiological and pharmacological activities.[21] In this paper, we offer a significant solution to the challenging chiral recognition of hydantoin derivatives, as five-membered N,N-heterocyclic compounds, with the discovery of a panel of remarkable tetraaza macrocyclic chiral solvating agents (TAMCSAs) that enable the determination of enantiomeric purity by means of ^{1}H NMR spectroscopy.

RESULTS AND DISCUSSION

TAMCSAs **1a–1c** were synthesized by intramolecular reductive coupling reaction of enantiopure diimines **3a–3c** (1 mmol), which were prepared according to our previously reported synthetic procedure,[22] with a dilute suspension (60 mL of dried DMF) of the activated Zn powder (0.65 g, 10 mmol) and MsOH (0.96 g, 10 mmol) in dried DMF (20 mL) for chiral recognition as chiral auxiliaries (Scheme 1).[23] Meanwhile, chiral compounds **2a–2c** were also obtained as intramolecular reductive products in 17–19% isolated yields.

All products were characterized by ^{1}H NMR, ^{13}C NMR, HRMS, and IR methods. Unfortunately, we were unable to obtain crystals of TAMCSAs **1a–1c**, suitable for X-ray singlecrystal diffraction. Therefore, their nuclear overhauser effect spectroscopy (NOESY) spectra were measured for assignment of absolute configuration of the two newly generated chiral carbon atoms (Ar*CH*NH) of TAMCSAs **1a–1c**. Their spectra show that the two types of protons of the Ar*CH*NH and CO*CH*Bn (phenylalanine moiety) groups of TAMCSAs **1a–1c** are located on the same side of the macrocyclic framework, as determined by the NOESY correlated ^{1}H NMR signals between the two types of protons (Ar*CH*NH and CO*CH*Bn). Based on the known absolute configuration (R) of CO*CH*Bn and the C_2-symmetric geometry, the absolute configuration of 5- and 6-carbon atoms (Ar*CH*NH) of TAMCSAs *1a–1c* is assigned as S and S-configurations (Scheme 1). Detailed NOESY spectra are available in the Supporting Information (Figures S5, S9, and S13).

As shown in Scheme 1, the multiple potential hydrogen bonding sites, such as amino, amide, and phenolic hydroxyl groups, featured in the molecular structure of TAMCSAs **1a–1c**, are the most distinguished structural elements, along with a C_2-symmetry and a 12-membered cavity.

Meanwhile, the enantiomers of hydantoin derivatives G**1–14**, as five-membered N,N-heterocycles, were directly prepared from the corresponding L- and D-amino acids (5.5 mmol, 1.1 equiv) in NaOH solution (1 M, 5 mL) with *p*-tolyl isocyanate (5 mmol) and 3,5-bis(trifluoromethyl)phenyl isocyanate (5 mmol) in CH_3CN (2 mL) in 50–89% isolated yields according to the related literature,[24] respectively (Scheme 2).

The new products were characterized by the spectroscopic methods noted above and by ^{19}F NMR spectroscopy (for new products containing CF_3 groups).

To explore the discrimination of enantiomers of hydantoin derivatives in the presence of TAMCSAs **1a–1c** by ^1H NMR spectroscopy, two samples of (±)-G**1** with TAMCSA **1a** (1:1 molar ratio, [5 mM]) and (±)-G**7** with TAMCSA **1c** (1:1 molar ratio, [10 mM]) were prepared in $CDCl_3$ based on the solubility, and their ^1H NMR spectra were measured on a 400 MHz spectrometer at 25 °C. The results show that enantiomers of (±)-G**1** and (±)-G**7** were remarkably differentiated by the split protons of CO*NH* and Ph*CH*$_3$ groups, respectively. Especially, a maximum nonequivalent chemical shift value ($\Delta\Delta\delta$) of the *NH* proton (CO*NH*) of (±)-G**7** has been established as 1.031 ppm, which is a sufficiently large nonequivalent chemical shift value in the field of chiral recognition by ^1H NMR chiral solvating agents. Subsequently, the assignments of enantiomers were determined by adding (*R*)-G**1** and (*R*)-G**7** to their corresponding samples note above. The ^1H NMR spectra of (±)-G**7** (a) and (±)-G**7** in the presence of TAMCSA **1c** (b), including partial expanded spectra and $\Delta\Delta\delta$ values of the split protons of CO*NH* and Ph*CH*$_3$, are shown in Figure 1.

Encouraged by these remarkable chiral discriminating results, we sought to further test and evaluate a range of chiral discriminating conditions, including concentration effects, the molar ratio of the host and guest, and a variety of deuterated solvents. In the end, $CDCl_3$ (in most cases) and a 1:1 molar ratio of the host/guest were adopted in this study. Different concentrations were used from 2.0 to 12.5 mM for obtaining clear ^1H NMR signals with as little overlapping and better baseline resolution peaks as possible. Detailed information is available (Table S1 and Figures S1 and S2).

Under optimized conditions, 40 samples of (±)-G**1**–**14** were prepared in the presence of TAMCSAs **1a–1c** in $CDCl_3$ or $CDCl_3$ containing 10% CD_3COCD_3 (three samples). Their ^1H NMR spectra were measured on a 400 or 600 MHz spectrometer at 25 °C, with the exception of (±)-G**1** with TAMCSA **1a** and (±)-G**7** with TAMCSA **1c**. The results indicate that the separated ^1H NMR signals of the multiple protons of (±)-G**1–14** were detected in the presence of TAMCSAs **1a–1c**. Subsequently, the assignments of enantiomers [(*S*)-GX (red ○) and (*R*)-GX (red ●), **X** = **1**–**7** and **9–13**; (*S,R*)-GX (red ○) and (*R,S*)-GX (red ●), **X** = **8** and **14**] were determined based on the aforementioned method. The $\Delta\Delta\delta$ values and partial ^1H NMR spectra of the *NH* proton (CO*NH*) of (±)-G**1–14**, as the representative protons, are summarized in Table 1.

As shown Table 1, all of the $\Delta\Delta\delta$ values of the split *NH* proton of (±)-G**1–14** exceed 0.1 ppm (from 0.167 to 1.309 ppm) in the TAMCSAs **1a–1c**. Furthermore, among them, a maximum $\Delta\Delta\delta$ value was observed at 1.309 ppm, which is unprecedented for the separated ^{1}H NMR signal in the field of chiral recognition by CSAs. In addition, compared with the $\Delta\Delta\delta$ values of the split proton of (±)-G**2** and (±)-G**3**, and (±)-G**7** and (±)-G**8**, the $\Delta\Delta\delta$ values of the corresponding protons of the (±)-G**11–14** with the 3,5-bis(trifluoromethyl)-phenyl group exhibited a clear tendency to become larger in most cases in the presence of the same chiral solvating agent, which may be the result of the electronic effect of the 3,5-bis(trifluoromethyl)phenyl substituent. Additional $\Delta\Delta\delta$ values of other protons and the ^{1}H NMR spectra of (±)-G**1–14** are shown in Table 2.

Stimulated by the highly significant discriminating results noted above, we strongly desired to explore interactions between the host and guest and the possible mechanism of chiral discrimination. First, Job plots[25] of (±)-G**1** with TAMCSA **1a** were achieved by ^{1}H NMR titration experiments. The results show that a maximum value ($X \times \Delta\delta_{SR}$ = 0.184 ppm, $X \times \Delta\delta_S$ = 0.255 ppm, and $X \times \Delta\delta_R$ = 0.071 ppm) of the *NH* proton (CO*NH*) of (±)-G**1** was observed at a molar fraction of X = 0.5. Meanwhile, a maximum value ($X \times \Delta\delta_{SR}$ = 0.011 ppm, $X \times \Delta\delta_S$ = 0.026 ppm, and $X \times \Delta\delta_R$ = 0.015 ppm) of Ph*CH* of (±)-G**1** was also exhibited at a molar fraction of X = 0.5 (Figure 2). The two results suggest that a pair of diastereoisomeric complexes with 1:1 stoichiometry is established between (±)-G**1** and TAMCSA **1a**.

In addition, to further understand the chiral discriminating behavior between the guest and host, the geometries of enantiomers (*S*)-G**1** and (*R*)-G**1** with TAMCSA **1a** were optimized using density functional theory (DFT) at the B3LYP/6-31G* level.[26] The continuum model (SMD) for chloroform was employed in all NMR calculations to simulate the effects of the solvent. All quantum chemical calculations were performed by the Gaussian 16 program package. The proposed models suggest that two pairs of hydrogen bonds between (*S*)-G**1** and (*R*)-G**1** with TAMCSA **1a** have been established. The hydrogen bonding interactions, CONH···OCNH (1.845 Å) and NHCO···HOC$_6$H$_4$ (1.748 Å) between (*S*)-G**1** and TAMCSA **1a** and CONH···OCNH (1.884 Å) and NHCO···HOC$_6$H$_4$ (1.749 Å) between (*R*)-G**1** and TAMCSA **1a**, are shown in Figure 3.

Additionally, the corresponding chemical shifts and non-equivalent chemical shifts obtained by DFT/SMD calculations are shown in Table 3.

The Cartesian coordinates and total energies (hartree) of the complexes of (*S*)-G**1** and (*R*)-G**1** with TAMCSA **1a** were obtained by means of B3LYP/6-31G* structural optimization (Tables S2–S6).

To further evaluate the intermolecular interaction between the host and guest, ^{1}H NMR titration of (*S*)-G**2** and (*R*)-G**2** with TAMCSA **1a** was performed, and their association constants (K_a) were calculated by the nonlinear curve-fitting method and are shown in Table 4.[27]

As shown in Table 4, it can be found that no significant differences between the association constants of (*S*)-G**2** and (*R*)-G**2** with TAMCSA **1a** may result from the differences in the geometry of the diastereoisomeric complexes, rather than the thermodynamic factors.

A highly remarkable chiral discrimination has thus been established by the split ^{1}H NMR peaks of multiple protons of hydantoin derivatives, in conjunction with sufficiently enough nonequivalent chemical shift values. Based on these excellent discriminating results, we ventured to explore another research goal of chiral recognition, namely, its application in the determination of ee of chiral analytes. For this purpose, samples of G**4** with different optical purities, containing (*S*)-G**4**% with 95.0, 90.0, 70.0, 50.0, 30.0, 5.0, and 0.0% ee, were prepared in the presence of TAMCSA **1a** in $CDCl_3$, and their ^{1}H NMR spectra were recorded on a 400 MHz spectrometer at 25 °C. Their ee values were calculated based on the integration of the *NH* proton (CO*NH*), featuring well-separated ^{1}H NMR signals and superior baseline resolution. The ee values for samples of high optical purity (up to 95% ee) were clearly elucidated by ^{1}H NMR spectra (Figure 4a). An excellent linear correlation between the theoretical (*X*) and observed (*Y*) % ee values was obtained (Figure 4c). To further verify this application, another set of samples of G**10** with different optical purities containing (*S*)-G**10**% with 90.0, 70.0, 50.0, 30.0, 5.0, and 0.0% ee was prepared in the presence of TAMCSA **1c**, and their ^{1}H NMR spectra were recorded on a 400 MHz spectrometer. Similar results (up to 90% ee) were obtained based on the aforementioned method and are shown in Figure 4b,d.

CONCLUSIONS

In conclusion, chiral recognition has been established by means of unprecedented nonequivalent chemical shift values (up to 1.309 ppm) of chiral hydantoin derivatives, in the presence of TAMCSAs **1a–1c** by ^{1}H NMR spectroscopy. In addition, better baseline resolution and clear ^{1}H NMR signals without overlapping peaks have been achieved. Their practical application in the determination of ee values has been established by accurate calculation of the integration area of the *NH* proton (CO*NH*) of G**4** (up to 95% ee) in the presence of TAMCSA **1a** and G**10** (up to 90% ee) in the presence of TAMCSA **1c**. Meanwhile, the intermolecular interaction between guests and hosts has been investigated by Job plots, association constants (K_a), and quantum chemical calculations. Most importantly, this work is highlighting the impact of the discrimination of enantiomers of chiral heterocyclic compounds and determination of ee values with the assistance of highly effective chiral solvating agents by ^{1}H NMR spectroscopy.

EXPERIMENTAL SECTION

General Information.

^{1}H NMR spectra and ^{13}C NMR were recorded on a Bruker Avance III spectrometer at 400 MHz and JEOL spectrometers at 400 and 600 MHz at 25 °C. The peak patterns are shown as the singlet (s), doublet (d), triplet (t), quartet (q), multiplet (m), and broad (br). HRMS spectra were acquired on AB SCIEX Triple TOF 5600+. IR spectra were obtained on a 360 Avatar FT-IR spectrometer as KBr pellets. Optical rotations were measured on a

PerkinElmer model 343 and Autopol III polarimeter using the sodium D line at 589 nm. All the solvents were dried by the standard procedure prior to use.

Synthesis of TAMCSAs 1a–1c.

To a solution of chiral diimines **3a–3c** (1 mmol) in dried DMF (60 mL) were added the activated zinc powder (0.65 g, 10 mmol) and MsOH (0.96 g, 10 mmol) in dried DMF (20 mL). The mixture was stirred for 23 h under a nitrogen atmosphere from −18 °C to rt. The reaction mixture was basified to pH = 10 with a saturated $NaHCO_3$ solution. The precipitate formed was filtered off and washed with $CHCl_3$. The organic layer was separated from the filtrate. The water layer was extracted with $CHCl_3$ (15 mL × 3). The combined organic phase was dried over anhydrous Na_2SO_4. The solvent was removed under reduced pressure, and the residue was purified by column chromatography on silica gel to afford TAMCSAs **1a–1c** in 17–25% yields and chiral compounds **2a–2c** in 17–19% yields.

(3R,5S,6S,8R,10aS, 14aS)-3,8-Dibenzyl-5,6-bis(2-hydroxy-5-methylphenyl)tetradecahydrobenzo[b][1, 4, 7, 10]-tetraazacydododecine-2,9-dione (TAMCSA 1a).—149 mg, 23% yield as a white solid. R_f = 0.3 (ethyl acetate/petroleum ether = 1/2). mp 186–188 °C. $[\alpha]_{20}^{D} = +64.8$ (c 0.01, $CHCl_3$). ^{1}H NMR (400 MHz, $CDCl_3$): δ 7.15–7.19 (m, 6H), 7.06–7.08 (m, 4H), 6.89 (dd, J = 8.20, 1.64 Hz, 2H), 6.81 (d, J = 8.12 Hz, 2H), 5.95 (s, 2H), 5.71 (d, J = 7.88 Hz, 2H), 4.32 (s, 2H), 3.68–3.73 (m, 2H), 3.28–3.32 (m, 2H), 2.93 (dd, J = 12.66, 9.78 Hz, 2H), 2.78 (dd, J = 12.68, 5.52 Hz, 2H), 2.01 (s, 6H), 1.62–1.64 (m, 2H), 1.24–1.27 (m, 2H), 1.11–1.16 (m, 2H), 0.90–0.96 (m, 2H). ^{13}C{^{1}H}NMR (100 MHz, $CDCl_3$): δ 173.7, 152.7, 136.7, 129.3, 128.6, 128.4, 128.3, 128.1, 126.7, 125.2, 116.8, 67.0, 61.6, 52.7, 40.1, 31.5, 24.6, 20.4. IR (KBr, cm^{-1}): 3286, 2936, 1655, 1560, 1500, 1455, 1260, 700. HRMS (ESI$^+$-TOF) m/z: [M + H]$^+$ calcd for $C_{40}H_{47}N_4O_4$, 647.3591; found, 647.3594.

(3R,5S,6S,8R,10aS, 14aS)-3,8-Dibenzyl-5,6-bis(2-hydroxy-3-methoxyphenyl)tetradecahydrobenzo[b][1, 4, 7, 10]-tetraazacyclododecine-2,9-dione (TAMCSA 1b).—115 mg, 17% yield as a white solid. R_f = 0.3 (ethyl acetate/petroleum ether = 2/3). mp 179–180 °C. $[\alpha]_{20}^{D} = +50.4$ (c 0.01, THF). ^{1}H NMR (400 MHz, $CDCl_3$): δ 7.12–7.19 (m, 6H), 7.08–7.10 (m, 4H), 6.71 (d, J = 8.04 Hz, 2H), 6.62 (t, J = 7.90 Hz, 2H), 6.37 (d, J = 7.28 Hz, 2H), 5.53 (br, 2H), 4.34 (s, 2H), 3.78 (s, 6H), 3.61–3.67 (m, 2H), 3.19–3.23 (m, 2H), 2.89–2.91 (m, 4H), 1.69 (br, 2H), 1.59–1.61 (m, 2H), 1.26–1.29 (m, 2H), 1.09–1.14 (m, 2H), 0.83–0.90 (m, 2H). ^{13}C{^{1}H} NMR (100 MHz, $CDCl_3$): δ 174.0, 147.4, 145.4, 137.1, 129.4, 128.3, 126.6, 124.2, 120.7, 118.5, 110.6, 66.8, 63.0, 56.0, 52.9, 40.1, 31.7, 24.7. IR (KBr, cm^{-1}): 3300, 2938, 1661, 1631, 1450, 1406, 1238, 1076, 697. HRMS (ESI$^+$-TOF) m/z: [M + H]$^+$ calcd for $C_{40}H_{47}N_4O_6$, 679.3490; found, 679.3465.

(3R,5S,6S,8R,10aS,14aS)-3,8-Dibenzyl-5,6-bis(2-hydroxy-4-methoxyphenyl)tetradecahydrobenzo[b][1, 4, 7, 10]-tetraazacyclododecine-2,9-dione (TAMCSA 1c).—170 mg, 25% yield as a white solid. R_f = 0.3 (ethyl acetate/petroleum ether = 2/3). mp 156–158 °C. $[\alpha]_{20}^{D} = +111.2$ (c 0.01, $CHCl_3$). ^{1}H NMR (400 MHz, $CDCl_3$):

δ 7.13–7.21 (m, 6H), 7.05–7.07 (m, 4H), 6.44 (s, 2H), 6.22–6.23 (m, 2H), 6.20–6.21 (m, 2H), 5.64 (s, 2H), 4.28 (s, 2H), 3.73 (s, 6H), 3.69–3.75 (m, 2H), 3.23–3.26 (m, 2H), 2.92 (dd, *J* = 12.36, 9.76 Hz, 2H), 2.82 (dd, *J* = 12.74, 5.54 Hz, 2H), 1.62–1.64 (m, 2H), 1.22–1.26 (m, 2H), 1.11–1.16 (m, 2H), 0.86–0.92 (m, 2H). $^{13}C\{^{1}H\}$ NMR (100 MHz, $CDCl_3$): δ 174.1, 159.6, 156.4, 136.7, 129.3, 129.0, 128.3, 126.6, 117.5, 105.2, 102.2, 66.6, 61.6, 55.0, 52.6, 40.1, 31.4, 24.6. IR (KBr, cm^{-1}): 3297, 2936, 1660, 1617, 1511, 1455, 1161, 700. HRMS (ESI^+-TOF) *m/z*: $[M + H]^+$ calcd for $C_{40}H_{47}N_4O_6$, 679.3490; found, 679.3488.

(2R,2′R)-N,N′-((1S,2S)-Cyclohexane-1,2-diyl)bis(2-((2-hydroxy-5-methylbenzyl)amino)-3-phenylpropanamide) (2a).—117 mg, 18% yield as a white solid. R_f = 0.3 (ethyl acetate/petroleum ether = 1/1). mp 172–174 °C. $[\alpha]_{20}^{D} = +51.7$ (*c* 0.01, $CHCl_3$). ^{1}H NMR (400 MHz, $CDCl_3$): δ 7.21–7.28 (m, 6H), 7.09–7.11 (m, 4H), 6.91 (dd, *J* = 8.16, 1.80 Hz, 2H), 6.70 (d, *J* = 8.12 Hz, 2H), 6.53 (d, *J* = 5.84 Hz, 2H), 6.49 (d, *J* = 1.6 Hz, 2H), 3.78 (d, *J* = 13.04 Hz, 2H), 3.50–3.53 (m, 2H), 3.46 (d, *J* = 13.04 Hz, 2H), 3.28 (t, *J* = 7.32 Hz, 2H), 2.98 (dd, *J* = 13.42, 7.02 Hz, 2H), 2.83 (dd, *J* = 13.4, 7.64 Hz, 2H), 2.09 (s, 6H), 1.79–1.82 (m, 2H), 1.64–1.66 (m, 5H), 1.19–1.24 (m, 2H), 0.90–0.98 (m, 2H). $^{13}C\{^{1}H\}$ NMR (100 MHz, $CDCl_3$): δ 173.7, 154.6, 136.9, 129.5, 129.4, 129.1, 128.8, 128.6, 127.0, 122.9, 116.2, 63.6, 53.4, 50.5, 40.1, 31.9, 24.4, 20.3. IR (KBr, cm^{-1}): 3299, 2933, 1647, 1629, 1550, 1499, 1252, 817, 699. HRMS (ESI^+-TOF) *m/z*: $[M + H]^+$ calcd for $C_{40}H_{49}N_4O_4$, 649.3748; found, 649.3750.

(2R,2′R)-N,N′-((1S,2S)-Cyclohexane-1,2-diyl)bis(2-((2-hydroxy-3-methoxybenzyl)amino)-3-phenylpropanamide) (2b).—129 mg, 19% yield as a white solid. R_f = 0.2 (ethyl acetate/petroleum ether = 2/3). mp 165—166 °C. $[\alpha]_{20}^{D} = +102.8$ (*c* 0.01, THF). ^{1}H NMR (400 MHz, $CDCl_3$): δ 7.42 (d, *J* = 6.56 Hz, 2H), 7.18–7.23 (m, 6H), 7.06–7.09 (m, 4H), 6.74 (dd, *J* = 8.16, 1.24 Hz, 2H), 6.63 (dd, *J* = 7.76, 7.92 Hz, 2H), 6.43 (dd, *J* = 7.60, 1.08 Hz, 2H), 3.85 (s, 6H), 3.81 (d, *J* = 12.84 Hz, 2H), 3.63—3.67 (m, 2H), 3.42 (d, *J* = 12.84 Hz, 2H), 3.29 (dd, *J* = 9.10, 5.30 Hz, 2H), 3.11 (dd, *J* = 13.70, 5.26 Hz, 2H), 2.65 (dd, *J* = 13.62, 9.18 Hz, 2H), 2.02–2.05 (m, 2H), 1.70–1.73 (m, 2H), 1.29–1.34 (m, 2H), 1.07–1.15 (m, 2H). $^{13}C\{^{1}H\}$ NMR (100 MHz, $CDCl_3$): δ 173.9, 147.2, 145.2, 137.3, 129.0, 128.6, 126.8, 124.1, 121.7, 119.2, 110.6, 63.2, 56.0, 52.9, 49.3, 40.1, 32.2, 24.6. IR (KBr, cm^{-1}): 3292, 2940, 2860, 1641, 1530, 1481, 1456, 1269, 1240, 1074, 733, 696. HRMS (ESI^+-TOF) *m/z*: $[M + H]^+$ calcd for $C_{40}H_{49}N_4O_6$, 681.3647; found, 681.3587.

(2R,2′R)-N,N′-((1S,2S)-Cyclohexane-1,2-diyl)bis(2-((2-hydroxy-4-methoxybenzyl)amino)-3-phenylpropanamide) (2c).—116 mg, 17% yield as a white solid. R_f = 0.3 (ethyl acetate/petroleum ether = 1/1). mp 186–188 °C. $[\alpha]_{20}^{D} = +69.9$ (*c* 0.01, $CHCl_3$). ^{1}H NMR (400 MHz, $CDCl_3$): δ 7.21–7.30 (m, 6H), 7.12–7.13 (m, 4H), 6.62 (d, *J* = 8.32 Hz, 2H), 6.38 (d, *J* = 2.48 Hz, 2H), 6.32 (d, *J* = 5.64 Hz, 2H), 6.23 (dd, *J* = 8.28, 2.52 Hz, 2H), 3.78 (d, *J* = 13.08 Hz, 2H), 3.72 (s, 6H), 3.46–3.49 (m, 4H), 3.27 (t, *J* = 7.32 Hz, 2H), 2.96 (dd, *J* = 13.42, 7.22 Hz, 2H), 2.87 (dd, *J* = 13.42, 7.42 Hz, 2H), 1.75–1.78 (m, 2H), 1.63–1.66 (m, 2H), 1.17–1.22 (m, 2H), 0.88–0.94 (m, 2H). $^{13}C\{^{1}H\}$ NMR (100 MHz, $CDCl_3$): δ 173.6, 160.6, 158.3, 136.9, 129.4, 129.1, 128.8, 127.0, 115.2, 105.1, 102.3, 63.2, 55.2, 53.7,

50.0, 40.1, 31.8, 24.4. IR (KBr, cm^{-1}): 3330, 3303, 1633, 1535, 1508, 1204, 1160, 1106, 699. HRMS (ESI^+-TOF) *m/z*: $[M + H]^+$ calcd for $C_{40}H_{49}N_4O_6$, 681.3647; found, 681.3659.

Synthesis of Enantiomrs of Hydantoin Derivatives G1–14.

To D- or L-amino acid (5.5 mmol, 1.1 equiv) in NaOH solution (1 M, 5 mL) was dropwise added the corresponding isocyanate (5 mmol) in CH_3CN (2 mL) at 0 °C. 1,4-Dioxane (5 mL) was added to the reaction solution after the mixture was stirred for 3 h. It was acidified to pH = 2 with concd hydrochloric acid after the reaction mixture was stirred for 8 h at room temperature. The mixture was stirred again for 10 h at 110 °C using a lab heating mantle. After cooling, the reaction mixture was extracted with EtOAc (10 mL × 3), and the combined organic phase was dried over anhydrous Na_2SO_4. The solvent was removed under reduced pressure, and the residue was purified by column chromatography on silica gel to afford the corresponding enantiomers of hydantoin derivatives G**1**–**14** in 50–89% yields.

(S)-5-Phenyl-3-(p-tolyl)imidazolidine-2,4-dione ((S)-G1).—1.07 g, 85% yield as a white solid. R_f = 0.3 (ethyl acetate/petroleum ether = 2/3). mp 240–243 °C. $[\alpha]_{20}^{D} = -5.4$ (*c* 0.01, DMSO). ^1H NMR (400 MHz, $CDCl_3$): δ 7.42–7.44 (m, 5H), 7.26 (s, 3H), 6.28 (s, 1H), 5.19 (s, 1H), 2.37 (s, 3H). $^{13}C\{^1H\}$ NMR (100 MHz, $CDCl_3$): δ 171.0, 157.0, 134.2, 129.8, 129.2, 128.6, 126.5, 126.1, 60.6, 21.2. IR (KBr, cm^{-1}): 2915, 1713, 1515, 1430, 1176, 810, 708. HRMS (ESI^+-TOF) *m/z*: $[M + H]^+$ calcd for $C_{16}H_{15}N_2O_2$, 267.1128; found, 267.1126.

(R)-5-Phenyl-3-(p-tolyl)imidazolidine-2,4-dione ((R)-G1).—1.10 g, 87% yield as a white solid. R_f = 0.3 (ethyl acetate/petroleum ether = 2:3). mp 242–246 °C. $[\alpha]_{20}^{D} = +5.6$ (*c* 0.01, DMSO). ^1H NMR (400 MHz, $CDCl_3$): δ 7.42–7.45 (m, 5H), 7.26 (s, 3H), 6.29 (s, 1H), 5.19 (s, 1H), 2.37 (s, 3H). $^{13}C\{^1H\}$ NMR (100 MHz, $CDCl_3$): δ 171.0, 156.9, 138.5, 134.2, 129.8, 129.2, 128.6, 126.5, 126.1, 60.6, 21.2. IR (KBr, cm^{-1}): 2915, 1713, 1515, 1425, 1176, 810, 708. HRMS (ESI^+-TOF) *m/z*: $[M + H]^+$ calcd for $C_{16}H_{15}N_2O_2$, 267.1128; found, 267.1126.

(R)-5-Benzyl-3-(p-tolyl)imidazolidine-2,4-dione ((R)-G2).—1.07 g, 80% yield as a white solid. R_f = 0.3 (ethyl acetate/petroleum ether = 1:1). mp 119–120 °C. $[\alpha]_{20}^{D} = +194.7$ (*c* 0.01, CH_3OH). ^1H NMR (400 MHz, $CDCl_3$): δ 7.28–7.33 (m, 3H), 7.21–7.25 (m, 4H), 7.04 (d, *J* = 8.20 Hz, 2H), 6.33 (s, 1H), 4.35–4.38 (m, 1H), 3.05 (dd, *J* = 13.90, 3.82 Hz, 1H), 3.05 (dd, *J* = 13.86, 7.34 Hz, 1H), 2.36 (s, 3H). $^{13}C\{^1H\}$ NMR (100 MHz, $CDCl_3$): δ 172.2, 156.5, 138.5, 134.7, 129.8, 129.5, 128.8, 128.6, 127.5, 126.1, 58.1, 37.9, 21.2. IR (KBr, cm^{-1}): 3288, 1724, 1476, 1419, 1278, 1137, 894, 702. HRMS (ESI^+-TOF) *m/z*: $[M + H]^+$ calcd for $C_{17}H_{17}N_2O_2$, 281.1284; found, 281.1289.

(R)-5-Methyl-3-(p-tolyl)imidazolidine-2,4-dione ((R)-G3).—0.75 g, 79% yield as a white solid. R_f = 0.2 (ethyl acetate/petroleum ether = 1:1). mp 150–153 °C. $[\alpha]_{20}^{D} = +32.5$ (*c* 0.01, CH_3OH). ^1H NMR (400 MHz, $CDCl_3$): δ 7.27 (br, 4H), 6.33 (s, 1H), 4.21–4.23 (m, 1H), 2.38 (s, 3H), 1.54 (d, *J* = 6.36 Hz, 3H). $^{13}C\{^1H\}$ NMR (100 MHz, $CDCl_3$): δ 173.7, 156.8, 138.5, 129.8, 128.7, 126.1, 52.9, 21.2, 17.8, IR (KBr, cm^{-1}): 3232, 1713, 1520, 1430,

1188, 815, 770. HRMS (ESI$^+$-TOF) *m/z*: [M + H]$^+$ calcd for $C_{11}H_{13}N_2O_2$, 205.0971; found, 205.0973.

(R)-5-Isopropyl-3-(p-tolyl)imidazolidine-2,4-dione ((R)-G4).—0.93 g, 85% yield as a white solid. R_f = 0.3 (ethyl acetate/petroleum ether = 2:3). mp 170–173 °C. $[\alpha]_{20}^{D}$ = + 96.6 (*c* 0.01, CH_3OH). ^{1}H NMR (400 MHz, $CDCl_3$): δ 7.25 (br, 4H), 6.06 (br, 1H), 4.05–4.06 (m, 1H), 2.38 (s, 3H), 2.32–2.33 (m, 1H), 1.09 (d, *J* = 6.84 Hz, 3H), 1.01 (d, *J* = 6.64 Hz, 3H). ^{13}C{^{1}H} NMR (100 MHz, $CDCl_3$): δ 166.8, 151.6, 132.6, 124.0, 123.0, 120.3, 56.4, 24.8, 15.4, 12.9, 10.2. IR (KBr, cm^{-1}): 3226, 1770, 1713, 1515, 1425, 1176, 787, 764. HRMS (ESI$^+$-TOF) *m/z*: [M + H]$^+$ calcd for $C_{13}H_{17}N_2O_2$, 233.1284; found, 233.1286.

(S)-5-Isobutyl-3-(p-tolyl)imidazolidine-2,4-dione ((S)-G5).—0.80 g, 69% yield as a white solid. R_f = 0.3 (ethyl acetate/petroleum ether = 2:3). mp 136–138 °C. $[\alpha]_{20}^{D}$ = − 78.3 (*c* 0.01, CH_3OH). ^{1}H NMR (400 MHz, $CDCl_3$): δ 7.26 (br, 4H), 6.00 (br, 1H), 4.17–4.19 (m, 1H), 2.38 (s, 3H), 1.85–1.89 (m, 2H), 1.65–1.68 (m, 1H), 1.00 (2d, *J* = 6.68, 7.36 Hz, 6H). ^{13}C{^{1}H} NMR (100 MHz, $CDCl_3$): δ 173.5, 156.8, 138.3, 129.7, 128.8, 126.0, 55.7, 41.0, 25.1, 23.0, 21.7, 21.2. IR (KBr, cm^{-1}): 3254, 2955, 1719, 1515, 1413, 1170, 815, 753. HRMS (ESI$^+$-TOF) *m/z*: [M + H]$^+$ calcd for $C_{14}H_{19}N_2O_2$, 247.1441; found, 247.1438.

(R)-5-Isobutyl-3-(p-tolyl)imidazolidine-2,4-dione ((R)-G5).—0.87 g, 75% yield as a white solid. R_f = 0.3 (ethyl acetate/petroleum ether = 2:3). mp 136–138 °C. $[\alpha]_{20}^{D}$ = + 78.5 (*c* 0.01, CH_3OH). ^{1}H NMR (400 MHz, $CDCl_3$): δ 7.26 (br, 4H), 6.16 (br, 1H), 4.17–4.19 (m, 1H), 2.38 (s, 3H), 1.85–1.89 (m, 2H), 1.65–1.68 (m, 1H), 1.00 (2d, *J* = 7.12, 6.96 Hz, 6H). ^{13}C{^{1}H} NMR (100 MHz, $CDCl_3$): δ 173.5, 156.9, 138.3, 129.8, 128.8, 126.0, 55.7, 25.1, 23.0, 21.7, 21.2. IR (KBr, cm^{-1}): 3254, 2955, 1719, 1515, 1413, 1171, 821, 747. HRMS (ESI$^+$-TOF) *m/z*: [M + H]$^+$ calcd for $C_{14}H_{19}N_2O_2$, 247.1441; found, 247.1443.

(S)-5-(2-(Methylthio)ethyl)-3-(p-tolyl)imidazolidine-2,4-dione ((S)-G6).—0.99 g, 79% yield as a white solid. R_f = 0.3 (ethyl acetate/petroleum ether = 1:1). mp 109–111 °C. $[\alpha]_{20}^{D}$ = − 53.9 (*c* 0.01, CH_3OH). ^{1}H NMR (400 MHz, $CDCl_3$): δ 7.27 (br, 4H), 6.49 (br, 1H), 4.28–4.31 (m, 1H), 2.67–2.71 (m, 2H), 2.38 (s, 3H), 2.28–2.34 (m, 1H), 2.12 (s, 3H), 2.04–2.10 (m, 1H). ^{13}C{^{1}H} NMR (100 MHz, $CDCl_3$): δ 172.8, 156.7, 138.4, 130.0, 128.7, 126.0, 56.3, 30.5, 30.1, 21.2, 15.3. IR (KBr, cm^{-1}): 3277, 2915, 1781, 1713, 1515, 1425, 1188, 815, 674. HRMS (ESI$^+$-TOF) *m/z*: [M + H]$^+$ calcd for $C_{13}H_{17}N_2O_2S$, 265.1005; found, 265.1007.

(R)-5-(2-(Methylthio)ethyl)-3-(p-tolyl)imidazolidine-2,4-dione ((R)-G6).—1.11 g, 89% yield as a white solid. R_f = 0.3 (ethyl acetate/petroleum ether = 1:1). mp 107–108 °C. $[\alpha]_{20}^{D}$ = + 54.2 (*c* 0.01, CH_3OH). ^{1}H NMR (400 MHz, $CDCl_3$): δ 7.27 (br, 4H), 6.39 (br, 1H), 4.29–4.31 (m, 1H), 2.68–2.71 (m, 2H), 2.38 (s, 3H), 2.29–2.33 (m, 1H), 2.12 (s, 3H), 2.06–2.10 (m, 1H). ^{13}C{^{1}H} NMR (100 MHz, $CDCl_3$): δ 172.8, 156.8, 138.4, 129.8, 128.7, 126.0, 56.3, 30.5, 30.1, 21.2, 15.3. IR (KBr, cm^{-1}): 3277, 2916, 1781, 1713, 1515, 1425, 1188, 821, 674. HRMS (ESI$^+$-TOF) *m/z*: [M + H]$^+$ calcd for $C_{13}H_{17}N_2O_2S$, 265.1005; found, 265.1003.

(S)-5-(Hydroxymethyl)-3-(p-tolyl)imidazolidine-2,4-dione ((S)-G7).—0.88 g, 85% yield as a white solid. R_f = 0.2 (ethyl acetate/petroleum ether = 8:1). mp 168–170 °C. $[\alpha]_{20}^{D}$ = + 99.8 (*c* 0.01, DMF). ^{1}H NMR (400 MHz, $CDCl_3$): δ 7.26 (br, 4H), 6.04 (br, 1H), 4.25–4.27 (m, 1H), 3.96–4.01 (m, 2H), 2.38 (s, 4H). ^{13}C{^{1}H} NMR (100 MHz, CD_3OD): δ 172.8, 157.7, 138.1, 129.4, 129.2, 126.4, 60.4, 59.5, 19.8. IR (KBr, cm^{-1}): 3260, 2916, 1713, 1520, 1425, 1334, 1171, 776. HRMS (ESI^+-TOF) *m/z*: $[M + H]^+$ calcd for $C_{11}H_{13}N_2O_3$, 221.0920; found, 221.0923.

(R)-5-(Hydroxymethyl)-3-(p-tolyl)imidazolidine-2,4-dione ((R)-G7).—0.89 g, 86% yield as a white solid. R_f = 0.2 (ethyl acetate/petroleum ether = 8:1). mp 168–170 °C. $[\alpha]_{20}^{D}$ = + 98.7 (*c* 0.01, DMF). ^{1}H NMR (400 MHz, $CDCl_3$): δ 7.26 (br, 4H), 6.18 (br, 1H), 4.24–4.26 (m, 1H), 3.94–4.00 (m, 2H), 2.50 (br, 1H), 2.38 (s, 3H). ^{13}C{^{1}H} NMR (100 MHz, CD_3OD): δ 172.8, 157.7, 138.1, 129.4, 129.2, 126.4, 60.4, 59.5, 19.8. IR (KBr, cm^{-1}): 3328, 2921, 1775, 1713, 1521, 1425, 1176, 680. HRMS (ESI^+-TOF) *m/z*: $[M + H]^+$ calcd for $C_{11}H_{13}N_2O_3$, 221.0920; found, 221.0919.

(S)-5-((R)-1-Hydroxyethyl)-3-(p-tolyl)imidazolidine-2,4-dione ((S,R)-G8).—0.87 g, 79% yield as a white solid. R_f = 0.3 (ethyl acetate/petroleum ether = 6:1). mp 176–178 °C. $[\alpha]_{20}^{D}$ = − 122.9 (*c* 0.01, DMF). ^{1}H NMR (400 MHz, $CDCl_3$): δ 7.22–7.27 (m, 4H), 6.55 (s, 1H), 4.21 (br, 1H), 4.01–4.03 (m, 1H), 2.64 (br, 1H), 2.37 (s, 3H), 1.34 (d, *J* = 6.52 Hz, 3H). ^{13}C{^{1}H} NMR (100 MHz, CD_3OD): δ 173.0, 157.9, 138.1, 129.4, 129.2, 126.4, 66.3, 62.9, 19.8, 18.9. IR (KBr, cm^{-1}): 3305, 1781, 1719, 1515, 1425, 1182, 810. HRMS (ESI^+-TOF) *m/z*: $[M + H]^+$ calcd for $C_{12}H_{15}N_2O_3$, 235.1077; found, 235.1081.

(R)-5-((S)-1-Hydroxyethyl)-3-(p-tolyl)imidazolidine-2,4-dione ((R,S)-G8).—0.97 g, 88% yield as a white solid. R_f = 0.3 (ethyl acetate/petroleum ether = 6:1). mp 174–176 °C. $[\alpha]_{20}^{D}$ = + 121.1 (*c* 0.01, DMF). ^{1}H NMR (400 MHz, $CDCl_3$): δ 7.22–7.25 (m, 4H), 6.64 (s, 1H), 4.20 (br, 1H), 4.00–4.01 (m, 1H), 2.71–2.73 (m, 1H), 2.37 (s, 3H), 1.33 (d, *J* = 6.44 Hz, 3H). ^{13}C{^{1}H} NMR (100 MHz, CD_3OD): δ 173.0, 157.9, 138.1, 129.4, 129.2, 126.4, 66.3, 62.9, 19.8, 18.9. IR (KBr, cm^{-1}): 3305, 1781, 1719, 1515, 1425, 1182, 810. HRMS (ESI^+-TOF) *m/z*: $[M + H]^+$ calcd for $C_{12}H_{15}N_2O_3$, 235.1077; found, 235.1074.

(*S*)-5-(4-Hydroxybenzyl)-3-(p-tolyl)imidazolidine-2,4-dione ((S)-G9).—1.16 g, 82% yield as a white solid. R_f = 0.2 (ethyl acetate/petroleum ether = 1:1). mp 80–83 °C. $[\alpha]_{20}^{D}$ = − 158.0 (*c* 0.01, DMF). ^{1}H NMR (400 MHz, $CDCl_3$): δ 7.22 (d, *J* = 8.08 Hz, 2H), 7.04–7.08 (m, 4H), 6.71 (d, *J* = 8.48 Hz, 2H), 6.03 (br, 1H), 5.48 (s, 1H), 4.35–4.38 (m, 1H), 3.18 (dd, *J* = 14.12, 4.04 Hz, 1H), 3.02 (dd, *J* = 14.12, 6.92 Hz, 1H), 2.35 (s, 3H). ^{13}C{^{1}H} NMR (100 MHz, $CDCl_3$): δ 172.8, 157.3, 155.3, 138.8, 130.8, 129.9, 128.3, 126.3, 125.7, 115.6, 58.3, 36.5, 21.1. IR (KBr, cm^{-1}): 3316, 1782, 1713, 1515, 1420, 1170, 815. HRMS (ESI^+-TOF) *m/z*: $[M + H]^+$ calcd for $C_{17}H_{17}N_2O_3$, 297.1233; found, 297.1236.

(R)-5-(4-Hydroxybenzyl)-3-(p-tolyl)imidazolidine-2,4-dione ((R)-G9).—1.17 g, 83% yield as a white solid. R_f = 0.2 (ethyl acetate/petroleum ether = 1:1). mp 82–84 °C. $[\alpha]_{20}^{D}$ = + 158.8 (*c* 0.01, DMF). ^{1}H NMR (400 MHz, $CDCl_3$): δ 7.21 (d, *J* = 8.00 Hz, 2H),

7.02–7.05 (m, 4H), 6.67 (d, J = 8.56 Hz, 2H), 6.27 (s, 1H), 5.82 (br, 1H), 4.34–4.38 (m, 1H), 3.14 (dd, J = 14.10, 4.14 Hz, 1H), 3.03 (dd, J = 14.12, 6.52 Hz, 1H), 2.34 (s, 3H). $^{13}C\{^1H\}$ NMR (100 MHz, $CDCl_3$): δ 172.8, 157.3, 155.3, 138.8, 130.8, 129.9, 128.3, 126.3, 125.7, 115.6, 58.3, 36.5, 21.1. IR (KBr, cm^{-1}): 3322, 1781, 1509, 1430, 1171, 815. HRMS (ESI^+-TOF) *m/z*: $[M + H]^+$ calcd for $C_{17}H_{17}N_2O_3$, 297.1233; found, 297.1237.

(S)-5-((1H-Indol-3-yl)methyl)-3-(p-tolyl)imidazolidine-2,4-dione((S)-G10).—1.28 g, 80% yield as a white solid. R_f = 0.3 (ethyl acetate/petroleum ether = 2:1). mp 92–95 °C. $[\alpha]_{20}^{D}$ = − 107.4 (c 0.01, DMF). ^1H NMR (400 MHz, $CDCl_3$): δ 8.08 (s, 1H), 7.65 (d, J = 7.88 Hz, 1H), 7.36 (d, J = 8.12 Hz, 1H), 7.20–7.23 (m, 3H), 7.15 (t, J = 7.50 Hz, 1H), 7.04–7.06 (m, 3H), 5.75 (s, 1H), 4.42–4.45 (m, 1H), 3.49 (dd, J = 14.72, 3.76 Hz, 1H), 3.19 (dd, J = 14.68, 8.28 Hz, 1H), 2.35 (s, 3H). $^{13}C\{^1H\}$ NMR (100 MHz, $CDCl_3$): δ 172.7, 156.6, 138.4, 136.2, 129.7, 128.7, 127.0, 126.1, 123.4, 122.5, 119.9, 118.7, 111.4, 109.0, 57.7, 28.0, 21.2. IR (KBr, cm^{-1}): 3345, 1770, 1708, 1509, 1425, 1188, 815, 742. HRMS (ESI^+-TOF) *m/z*: $[M + H]^+$ calcd for $C_{19}H_{18}N_3O_2$, 320.1393; found, 320.1394.

(R)-5-((1 H-Indol-3-yl)methyl)-3-(p-tolyl)imidazolidine-2,4-dione ((R)-G10).—1.28 g, 80% yield as a white solid. R_f = 0.3 (ethyl acetate/petroleum ether = 2:1). mp 92–96 °C. $[\alpha]_{20}^{D}$ = + 107.5 (c 0.01, DMF). ^1H NMR (400 MHz, $CDCl_3$): δ 8.08 (s, 1H), 7.64 (d, J = 8.00 Hz, 1H), 7.35 (d, J = 8.04 Hz, 1H), 7.20–7.23 (m, 3H), 7.15 (t, J = 7.23 Hz, 1H), 7.02–7.05 (m, 3H), 5.84 (s, 1H), 4.41–4.44 (m, 1H), 3.47 (dd, J = 14.70, 3.70 Hz, 1H), 3.18 (dd, J = 14.70, 8.18 Hz, 1H), 2.35 (s, 3H). $^{13}C\{^1H\}$ NMR (100 MHz, $CDCl_3$): δ 172.8, 156.8, 138.4, 136.2, 129.7, 128.6, 127.0, 126.1, 123.5, 122.4, 119.8, 118.7, 111.4, 108.9, 57.7, 27.9, 21.1. IR (KBr, cm^{-1}): 3345, 1770, 1713, 1515, 1419, 1176, 810, 748. HRMS (ESI^+-TOF) *m/z*: $[M + H]^+$ calcd for $C_{19}H_{18}N_3O_2$, 320.1393; found, 320.1395.

(S)-5-Benzyl-3-(3,5-bis(trifluoromethyl)phenyl)imidazolidine-2,4-dione ((S)-G11).—1.11 g, 55% yield as a white solid. R_f = 0.3 (ethyl acetate/petroleum ether = 1:4). mp 110–111 °C. $[\alpha]_{20}^{D}$ = − 101.2 (c 0.01, DMF). ^1H NMR (400 MHz, $CDCl_3$): δ 7.85 (s, 1H), 7.78 (s, 2H), 7.30–7.36 (m, 3H), 7.24–7.26 (m, 2H), 5.82 (s, 1H), 4.47–4.49 (m, 1H), 3.35 (dd, J = 13.86, 3.10 Hz, 1H), 3.08 (dd, J = 13.94, 7.82 Hz, 1H). $^{13}C\{^1H\}$ NMR (100 MHz, $CDCl_3$): δ 171.1, 154.9, 134.1, 132.9, 132.5 (q, J = 33.9 Hz), 129.4, 129.0, 127.9, 126.0–126.8 (m), 122.8 (q, J = 269.7 Hz), 121.7(5)-121.8 (m), 58.2, 38.1. ^{19}F NMR (376 MHz, $CDCl_3$): δ −62.8. IR (KBr, cm^{-1}): 3299, 1790, 1726, 1476, 1418, 1279, 1184, 112, 895, 700. HRMS (ESI^+-TOF) *m/z*: $[M + H]^+$ calcd for $C_{18}H_{13}N_2O_2F_6$, 403.0875; found, 403.0879.

(R)-5-Benzyl-3-(3,5-bis(trifluoromethyl)phenyl)imidazolidine-2,4-dione ((R)-G11).—1.05 g, 52% yield as a white solid. R_f = 0.3 (ethyl acetate/petroleum ether = 1:4). mp 110–111 °C. $[\alpha]_{20}^{D}$ = + 99.5 (c 0.01, DMF). ^1H NMR (400 MHz, $CDCl_3$): δ 7.85 (s, 1H), 7.77 (s, 2H), 7.30–7.38 (m, 3H), 7.24–7.26 (m, 2H), 5.89 (s, 1H), 4.47–4.50 (m, 1H), 3.34 (dd, J = 13.92, 3.72 Hz, 1H), 3.08 (dd, J = 13.96, 7.80 Hz, 1H). $^{13}C\{^1H\}$ NMR (100 MHz, $CDCl_3$): δ 171.4, 155.6, 134.1, 132.9, 132.5 (q, J = 33.9 Hz), 129.6, 128.9, 127.9, 126.1–126.1(2) (m), 122.8 (q, J = 271.5 Hz), 121.8–121.9 (m), 58.2, 38.0. ^{19}F NMR (376

MHz, $CDCl_3$): δ −62.8. IR (KBr, cm^{-1}): 3285, 1780, 1728, 1448, 1416, 1279, 1179, 1132, 895, 698. HRMS (ESI^+-TOF) *m/z*: $[M + H]^+$ calcd for $C_{18}H_{13}N_2O_2F_6$, 403.0875; found, 403.0880.

(S)-3-(3,5-Bis(trifluoromethyl)phenyl)-5-methylimidazolidine-2,4-dione ((S)-G12).—0.88 g, 54% yield as a white solid. R_f = 0.3 (ethyl acetate/petroleum ether = 1:2). mp 90–91 °C. $[\alpha]_{20}^{D} = -21.5$ (*c* 0.01, DMF). ^1H NMR (400 MHz, $CDCl_3$): δ 8.04 (s, 1H), 7.88 (s, 2H), 6.43 (br, 1H), 4.30–4.35 (m, 1H), 1.60 (d, *J* = 6.92 Hz, 3H). $^{13}C\{^1H\}$ NMR (100 MHz, $CDCl_3$): δ 172.5, 155.0, 133.2, 132.5 (q, *J* = 33.9 Hz), 125.7–125.7(5) (m), 122.8 (q, *J* = 271.5 Hz), 121.5(5)–121.6 (m), 52.9, 17.8. ^{19}F NMR (376 MHz, $CDCl_3$): δ −62.8. IR (KBr, cm^{-1}): 3316, 1787, 1730, 1476, 1413, 1278, 1176, 1137, 894, 680; HRMS (ESI^+-TOF) *m/z*: $[M + H]^+$ calcd for $C_{12}H_9N_2O_2F_6$, 327.0562; found, 327.0559.

(R)-3-(3,5-Bis(trifluoromethyl)phenyl)-5-methylimidazolidine-2,4-dione ((R)-G12).—0.82 g, 50% yield as a white solid. R_f = 0.3 (ethyl acetate/petroleum ether = 1:2). mp 90–92 °C. $[\alpha]_{20}^{D} = +22.5$ (*c* 0.01, DMF). ^1H NMR (400 MHz, $CDCl_3$): δ 8.03 (s, 1H), 7.88 (s, 2H), 6.48 (br, 1H), 4.30–4.35 (m, 1H), 1.60 (d, *J* = 6.96 Hz, 3H). $^{13}C\{^1H\}$ NMR (100 MHz, $CDCl_3$): δ 172.6, 155.0, 133.2, 132.5 (q, *J* = 33.9 Hz), 125.7 (q, *J* = 3.4 Hz), 122.8 (q, *J* = 271.5 Hz), 121.5(5)–121.6 (m), 52.9, 17.8. ^{19}F NMR (376 MHz, $CDCl_3$): δ −62.8. IR (KBr, cm^{-1}): 3316, 1782, 1732, 1478, 1416, 1281, 1179, 1132, 893, 681. HRMS (ESI^+-TOF) *m/z*: $[M + H]^+$ calcd for $C_{12}H_9N_2O_2F_6$, 327.0562; found, 327.0556.

(S)-3-(3,5-Bis(trifluoromethyl)phenyl)-5-(hydroxymethyl)-imidazolidine-2,4-dione ((S)-G13).—0.91 g, 53% yield as a white solid. R_f = 0.3 (ethyl acetate/petroleum ether = 2:1). mp 134–136 °C. $[\alpha]_{20}^{D} = -57.6$ (*c* 0.01, DMF). ^1H NMR (400 MHz, $CDCl_3$): δ 8.02 (s, 2H), 7.89 (s, 1H), 6.13 (br, 1H), 4.35–4.37 (m, 1H), 4.03–4.12 (m, 2H), 2.28 (br, 1H). $^{13}C\{^1H\}$ NMR (100 MHz, CD_3OD): δ 171.8, 156.2, 134.2, 131.9 (q, *J* = 33.6 Hz), 126.1 (q, *J* = 3.9 Hz), 123.1 (q, *J* = 270.5 Hz), 120.6–120.8 (m), 60.3, 59.6. ^{19}F NMR (376 MHz, CD_3OD): δ −64.4. IR (KBr, cm^{-1}): 3418, 3260, 1787, 1724, 1476, 1419, 1278, 1188, 1131, 1075, 685. HRMS (ESI^+-TOF) *m/z*: $[M + H]^+$ calcd for $C_{12}H_9N_2O_3F_6$, 343.0511; found, 343.0509.

(R)-3-(3,5-Bis(trifluoromethyl)phenyl)-5-(hydroxymethyl)-imidazolidine-2,4-dione ((R)-G13).—0.92 g, 54% yield as a white solid. R^f = 0.3 (ethyl acetate/petroleum ether = 2:1). mp 132–133 °C. $[\alpha]_{20}^{D} = +57.8$ (*c* 0.01, DMF). ^1H NMR (400 MHz, $CDCl_3$): δ 8.02 (s, 2H), 7.88 (s, 1H), 6.21 (br, 1H), 4.36–4.38 (m, 1H), 4.04–4.14 (m, 2H), 2.28 (br, 1H). $^{13}C\{^1H\}$ NMR (100 MHz, CD_3OD): δ 171.8, 156.2, 134.2, 131.9 (q, *J* = 33.7 Hz), 126.1 (q, *J* = 3.8 Hz), 123.1 (q, *J* = 270.5 Hz), 120.7 (q, *J* = 3.8 Hz), 60.3, 59.6. ^{19}F NMR (376 MHz, CD_3OD): δ −64.3. IR (KBr, cm^{-1}): 3418, 3260, 1787, 1476, 1419, 1278, 1188, 1131, 1075, 889, 686. HRMS (ESI^+-TOf) *m/z*: $[M + H]^+$ calcd for $C_{12}H_9N_2O_3F_6$, 343.0511; found, 343.0512.

(S)-3-(3,5-Bis(trifluoromethyl)phenyl)-5-((R)-1-hydroxyethyl)-imidazolidine-2,4-dione ((S,R)-G14).—0.99 g, 56% yield as a white solid. R_f = 0.3 (ethyl acetate/petroleum

ether = 1:1). mp 178–180 °C. $[\alpha]_{20}^{D} = -83.1$ (c 0.01, DMF). ^{1}H NMR (400 MHz, $CDCl_3$): δ 8.02 (s, 2H), 7.87 (s, 1H), 5.84 (s, 1H), 4.26–4.34 (m, 1H), 4.13–4.14 (m, 1H), 1.94 (d, J = 6.68 Hz, 1H), 1.45 (d, J = 6.48 Hz, 3H). ^{13}C{^{1}H} NMR (100 MHz, CD_3OD): δ 172.0, 156.4, 134.2, 131.9 (q, J = 33.6 Hz), 126.1 (q, J = 3.5 Hz), 123.1 (q, J = 270.5 Hz), 120.6–120.7 (m), 66.3, 63.0, 18.9. ^{19}F NMR (376 MHz, CD_3OD): δ −64.3. IR (KBr, cm^{-1}): 3433, 3372, 1777, 1730, 1482, 1423, 1281, 1182, 1135, 1088, 890, 686; HRMS (ESI^{+}-TOF) *m/z*: $[M + H]^{+}$ calcd for $C_{13}H_{11}N_2O_3F_6$, 357.0668; found, 357.0669.

(R)-3-(3,5-Bis(trifluoromethyl)phenyl)-5-((S)-1-hydroxyethyl)-imidazolidine-2,4-dione ((R,S)-G14).—1.02 g, 57% yield as a white solid. R_f = 0.3 (ethyl acetate/petroleum ether = 1:1). mp 172–174 °C. $[\alpha]_{20}^{D} = +82.9$ (c 0.01, DMF). ^{1}H NMR (400 MHz, $CDCl_3$): δ 8.02 (s, 2H), 7.87 (s, 1H), 5.89 (s, 1H), 4.26–4.33 (m, 1H), 4.13–4.14 (m, 1H), 1.95 (d, J = 6.64 Hz, 1H), 1.45 (d, J = 6.48 Hz, 3H). ^{13}C{^{1}H} NMR (100 MHz, CD_3OD): δ 172.0, 156.4, 134.2, 131.9 (q, J = 33.6 Hz), 126.1–126.1(2) (m), 123.1 (q, J = 270.5 Hz), 120.6–120.7 (m), 66.3, 63.0, 18.9. ^{19}F NMR (376 MHz, CD_3OD): δ −64.4. IR (KBr, cm^{-1}): 3373, 1775, 1730, 1481, 1425, 1278, 1182, 1131, 1086, 894, 680. HRMS (ESI^{+}-TOF) *m/z*: $[M + H]^{+}$ calcd for $C_{13}H_{11}N_2O_3F_6$, 357.0668; found, 357.0667.

Supplementary Material

Refer to Web version on PubMed Central for supplementary material.

ACKNOWLEDGMENTS

This work was supported by the Scientific Research Fund Performance Award of Beijing Normal University (award number 10200/111203277). Work in the Missouri Lab (P.S.) was supported by the National Institute of General Medical Science of the National Institutes of Health under award number R15GM117508 and R15GM139071.

REFERENCES

(1). (a) Li M-L; Li Y; Pan J-B; Li Y-H; Song S; Zhu S-F; Zhou Q-L Carboxyl group-directed iridium-catalyzed enantioselective hydrogenation of aliphatic γ-ketoacids. ACS Catal. 2020, 10, 10032–10039.(b) Calcaterra A; D'Acquarica I The Market of chiral drugs: Chiral switches de novo enantiomerically pure compounds. J. Pharm. Biomed. Anal 2018, 147, 323–340. [PubMed: 28942107] (c) Glavin DP; Burton AS; Elsila JE; Aponte JC; Dworkin JP The search for chiral asymmetry as a potential biosignature in our solar system. Chem. Rev 2020, 120, 4660–4689. [PubMed: 31743015] (d) Wang Y; Zhao X; Yu Z; Xu Z; Zhao B; Ozaki Y A chiral-label-free SERS strategy for the synchronous chiral discrimination and identification of small aromatic molecules. Angew. Chem., Int. Ed 2020, 59, 19079–19086.

(2). (a) Höglund P; Eriksson T; Björkman S A double-blind study of the sedative effects of the thalidomide enantiomers in humans. J. Pharmcol. Biopharm 1998, 26, 363–383. (b) Tran CD; Oliveira D; Yu S Chiral ionic liquid that functions as both solvent and chiral selector for the determination of enantiomeric compositions of pharmaceutical products. Anal. Chem 2006, 78, 1349–1356. [PubMed: 16478133] (c) Zaremska V; Tan J; Lim S; Knoll W; Pelosi P Isoleucine residues determine chiral discrimination of odorant-binding protein. Chem.–Eur. J 2020, 26, 8720–8724. [PubMed: 32167603]

(3). (a) Pirkle WH; Pochapsky TC Considerations of chiral recognition relevant to the liquid chromatographic separation of enantiomers. Chem. Rev 1989, 89, 347–362. (b) Han SM Direct enantiomeric separations by high performance liquid chromatography using cyclodextrins. Biomed. Chromatogr 1997, 11, 259–271. [PubMed: 9376706] (c) Welch CJ Pirkle William H.: Stereochemistry pioneer. Chirality 2020, 32, 961–974. [PubMed: 32388884]

(4). (a) Flack HD; Bernardinelli G The use of X-ray crystallography to determine absolute configuration. Chirality 2008, 20, 681–690. [PubMed: 17924422] (b) Parsons S. Determination of absolute configuration using X-ray diffraction. Tetrahedron: Asymmetry 2017, 28, 1304–1313. (c) Gropp C; Husch T; Trapp N; Reiher M; Diederich F Hydrogen-bonded networks: Molecular recognition of cyclic alcohols in enantiopure alleno-acetylenic cage receptors. Angew. Chem., Int. Ed 2018, 57, 16296–16301.

(5). (a) De Los Santos ZA; Lynch CC; Wolf C Optical chirality sensing with an auxiliary-free earth-abundant cobalt probe. Angew. Chem., Int. Ed 2019, 58, 1198–1202. (b) Shimo S; Takahashi K; Iwasawa N 1,2-Dihydro-1-hydroxy-2,3,1-benzodiazaborine bearing an acridine moiety as a circular dichroism probe for determination of absolute configuration of mono-alcohols. Chem.–Eur. J 2019, 25, 3790–3794. [PubMed: 30689223] (c) Wang LL; Quan M; Yang TL; Chen Z; Jiang W A green and wide-scope approach for chiroptical sensing of organic molecules through biomimetic recognition in water. Angew. Chem., Int. Ed 2020, 59, 23817–23824.

(6). (a) Komori K; Taniguchi T; Mizutani S; Monde K; Kuramochi K; Tsubaki K Short synthesis of berkeleyamide D and determination of the absolute configuration by the vibrational circular dichroism exciton chirality method. Org. Lett 2014, 16, 1386–1389. [PubMed: 24527805] (b) Poopari MR; Dezhahang Z; Shen K; Wang L; Lowary TL; Xu Y Absolute configuration and conformation of two Fráter–Seebach alkylation reaction products by film VCD and ECD spectroscopic analyses. J. Org. Chem 2015, 80, 428–437. [PubMed: 25437116]

(7). (a) Parker D. NMR determination of enantiomeric purity. Chem. Rev 1991, 91, 1441–1457.(b) Yang G-H; Li Y; Li X Chirality sensing of molecules with diverse functional groups by using N-tert-butyl sulfinyl squaramide. Asian J. Org. Chem 2018, 7, 770–775.(c) Kuhn LT; Motiram-Corral K; Athersuch TJ; Parella T; Pérez-Trujillo M Simultaneous enantiospecific detection of multiple compounds in mixtures using NMR spectroscopy. Angew. Chem., Int. Ed 2020, 59, 23615–23619.(d) Li G-W; Wang X-J; Cui D-D; Zhang Y-F; Xu R-Y; Shi S-H; Liu L-T; Wang M-C; Liu H-M; Lei X-X Azaheterocyclic diphenylmethanol chiral solvating agents for the NMR chiral discrimination of alpha-substituted carboxylic acids. RSC Adv. 2020, 10, 34605–34611. [PubMed: 35514411] (e) Recchimurzo A; Micheletti C; Uccello-Barretta G; Balzano F A dimeric thiourea CSA for the enantiodiscrimination of amino acid derivatives by NMR spectroscopy. J. Org. Chem 2021, 86, 7381–7389. [PubMed: 34019407]

(8). (a) Sheykhi S; Mosca L; Durgala JM; Anzenbacher P Jr. An indicator displacement assay recognizes enantiomers of chiral carboxylates. Chem. Commun 2019, 55, 7183–7186.(b) Pu L. Enantioselective fluorescent recognition of free amino acids: challenges and opportunities. Angew. Chem., Int. Ed 2020, 59, 21814–21828.

(9). (a) Ito S; Okuno M; Asami M Differentiation of enantiomeric anions by NMR spectroscopy with chiral bisurea receptors. Org. Biomol Chem 2018, 16, 213–222. [PubMed: 29136083] (b) Kriegelstein M; Profous D; Přibylka A; Cankař P The assignment of the absolute configuration of β-chiral primary alcohols with axially chiral trifluoromethylbenzimidazolylbenzoic acid. J. Org. Chem 2020, 85, 12912–12921. [PubMed: 32881501]

(10). (a) Balzano F; Uccello-Barretta G; Aiello F Chiral analysis by NMR spectroscopy: chiral solvating agents. Chiral Analysis, 2nd ed.; Elsevier, 2018; pp 367–427.(b) Wenzel TJ Differentiation of Chiral Compounds Using NMR Spectroscopy, 2nd ed.; Wiley, 2018.

(11). (a) Labuta J; Hill JP; Ishihara S; Hanyková L; Ariga K Chiral sensing by nonchiral tetrapyrroles. Acc. Chem. Res 2015, 48, 521–529. [PubMed: 25734700] (b) Ema T; Yamasaki T; Watanabe S; Hiyoshi M; Takaishi K Cross-coupling approach to an array of macrocyclic receptors functioning as chiral solvating agents. J. Org. Chem 2018, 83, 10762–10769. [PubMed: 30126269]

(12). (a) Raval HB; Bedekar AV Synthesis and study of fluorine containing Kagan's amides as chiral solvating agents for enantiodiscrimination of acids by NMR spectroscopy. Chemistry Select 2020, 5, 6927–6932.(b) Prasad D; Mogurampelly S; Chaudhari SR *R*-VAPOL-phosphoric acid based ^{1}H and ^{13}C-NMR for sensing of chiral amines and acids. RSC Adv. 2020, 10, 2303–2312. [PubMed: 35494596] (c) Erol Gunal S; Teke Tuncel S; Dogan I Enantiodiscrimination of carboxylic acids using single enantiomer thioureas as chiral solvating agents. Tetrahedron 2020, 76, 131141–131146.(d) Recchimurzo A; Micheletti C; Uccello-Barretta G; Balzano F A dimeric thiourea CSA for the enantiodiscrimination of amino acid derivatives by NMR spectroscopy. J. Org. Chem 2021, 86, 7381–7389. [PubMed: 34019407]

(13). (a) Mishra SK; Chaudhari SR; Suryaprakash N *In situ* approach for testing the enantiopurity of chiral amines and amino alcohols by ^{1}H NMR. Org. Biomol. Chem 2014, 12, 495–502. [PubMed: 24280980] (b) Seo M-S; Kim H ^{1}H NMR chiral analysis of charged molecules via ion pairing with Aluminum complexes. J. Am. Chem. Soc 2015, 137, 14190–14195. [PubMed: 26479579] (c) Sun Z; Chen Z; Wang Y; Zhang X; Xu J; Bian G; Song L Chiral discrimination of varied ammonium compounds through ^{1}H NMR using a binuclear Ti complex sensor. Org. Lett 2020, 22, 589–593. [PubMed: 31913635]

(14). (a) Yang K; Li S-Z; Wang Y-H; Zhang W-Z; Xu Z-H; Zhou X-Y; Zhu R-X; Luo J; Wan Q Enantioselective recognition of an inherently chiral calix[4]arene crown-6 carboxylic acid cone conformer towards chiral aminoalcohols. RSC Adv. 2014, 4, 6517–6526.(b) Yang J; Chatelet B; Dufaud V; Hérault D; Jean M; Vanthuyne N; Mulatier J-C; Pitrat D; Guy L; Dutasta J-P; Martinez A Enantio- and substrates-selective recognition of chiral neurotransmitters with C_3-symmetric switchable receptors. Org. Lett 2020, 22, 891–895. [PubMed: 31985232]

(15). (a) Bian G; Yang S; Huang H; Zong H; Song L; Fan H; Sun X Chirality sensing of tertiary alcohols by a novel strong hydrogen-bonding donor–selenourea. Chem. Sci 2016, 7, 932–938. [PubMed: 29899892] (b) Seo M-S; Jang S; Kim H A chiral aluminum solvating agent (CASA) for ^{1}H NMR chiral analysis of alcohols at low temperature. Chem. Commun 2018, 54, 6804–6807.

(16). Chen Z; Fan H; Yang S; Bian G; Song L Chiral sensors for determining the absolute configurations of α-amino acids derivatives. Org. Biomol. Chem 2018, 16, 8311–8317. [PubMed: 30204200]

(17). (a) Bai L; Chen P; Xiang J; Sun J; Lei X Enantiomeric NMR discrimination of carboxylic acids using actinomycin D as a chiral solvating agent. Org. Biomol. Chem 2019, 17, 1466–1470. [PubMed: 30672950] (b) Malinowska M; Jarzyński S; Pieczonka A; Rachwalski M; Leśniak S; Zawisza A Optically pure aziridin-2-yl methanols as readily available ^{1}H NMR sensors for enantiodiscrimination of α-recemic carboxylic acids containing tertiary or quaternary stereogenic centers. J. Org. Chem 2020, 85, 11794–11801. [PubMed: 32805106]

(18). Jang S; Kim H Understanding the origin of the chiral recognition of esters with octahedral chiral cobalt complexes. Asian J. Org. Chem 2021, 10, 886–890.

(19). (a) Lv C-X; Feng L; Zhao H-M; Wang G; Stavropoulos P; Ai L Chiral discrimination of α-hydroxy acids and *N*-Ts-α-amino acids induced by tetraaza macrocyclic chiral solvating agents by using ^{1}H NMR spectroscopy. Org. Biomol. Chem 2017, 15, 1642–1650. [PubMed: 28127599] (b) Fang L-X; Lv C-X; Wang G; Feng L; Stavropoulos P; Gao G-P; Ai L; Zhang JX Discrimination of enantiomers of dipeptide derivatives with two chiral centers by tetraaza macrocyclic chiral solvating agents using ^{1}H NMR spectroscopy. Org. Chem. Front 2016, 3, 1716–1724. [PubMed: 28191319]

(20). Couffin A; Thillaye du Boullay O; Vedrenne M; Navarro C; Martin-Vaca B; Bourissou D Enantio-differentiation of *O*-heterocycles using a binol-derived disulfonimide as a chiral solvating agent. Chem. Commun 2014, 50, 5997–6000.

(21). (a) Nique F; Hebbe S; Peixoto C; Annoot D; Lefrançois J-M; Duval E; Michoux L; Triballeau N; Lemoullec J-M; Mollat P; Thauvin M; Prangé T; Minet D; Clément-Lacroix P; Robin-Jagerschmidt C; Fleury D; Guédin D; Deprez P Discovery of diarylhydantoins as new selective androgen receptor modulators. J. Med. Chem 2012, 55, 8225–8235. [PubMed: 22897611] (b) Ma B-D; Du S-H; Wang Y; Ou X-M; Huang M-Z; Wang L-X; Wang X-G Synthesis of chiral hydantoin derivatives by homogeneous Pd-catalyzed asymmetric hydrogenation. Tetrahedron: Asymmetry 2017, 28, 47–53.

(22). Feng L; Gao G-P; Zhao H-M; Zheng L; Wang Y; Stavropoulos P; Ai L; Zhang J-X Synthesis of tripeptide derivatives with three stereogenic centers and chiral recognition probed by tetrazaz macrocyclic chiral solvating agents derived from D-phenylalanine and (1*S*,2*S*)-(+)-1,2-diaminocyclohexane via ^{1}H NMR spectroscopy. J. Org. Chem 2018, 83, 13874–13887. [PubMed: 30346768]

(23). Kise N; Oike H; Okazaki E; Yoshimoto M; Shono T Synthesis of nitrogen-containing macrocycles with reductive intramolecular coupling of aromatic diimines. J. Org. Chem 1995, 60, 3980–3992.

(24). Wang C; Zhao Q; Vargas M; Jones JO; White KL; Shackleford DM; Chen G; Saunders J; Ng ACF; Chiu FCK; Dong Y; Charman SA; Keiser J; Vennerstrom JL Revisiting the SAR of the antischistosomal aryl hydantoin (RO 133978). J. Med. Chem 2016, 59, 10705–10718. [PubMed: 27933964]

(25). (a) Job P. Formation and stability of inorganic complexes in solution. Ann. Chim 1928, 9, 113–203.(b) Ulatowski F; Dąbrowa K; Bałakier T; Jurczak J Recognizing the limited applicability of Job plots in studying host-guest interactions in supramolecular chemistry. J. Org. Chem 2016, 81, 1746–1756. [PubMed: 26866984]

(26). Becke AD Density-functional thermochemistry. III. The role of exact exchange. J. Chem. Phys 1993, 98, 5648–5652.

(27). Uccello-Barretta G; Balzano F; Caporusso AM; Iodice A; Salvadori P Permethylated βcyclodextrin as chiral solvating agent for the NMR assignment of the absolute configuration of chiral trisubstituted allenes. J. Org. Chem 1995, 60, 2227–2231.

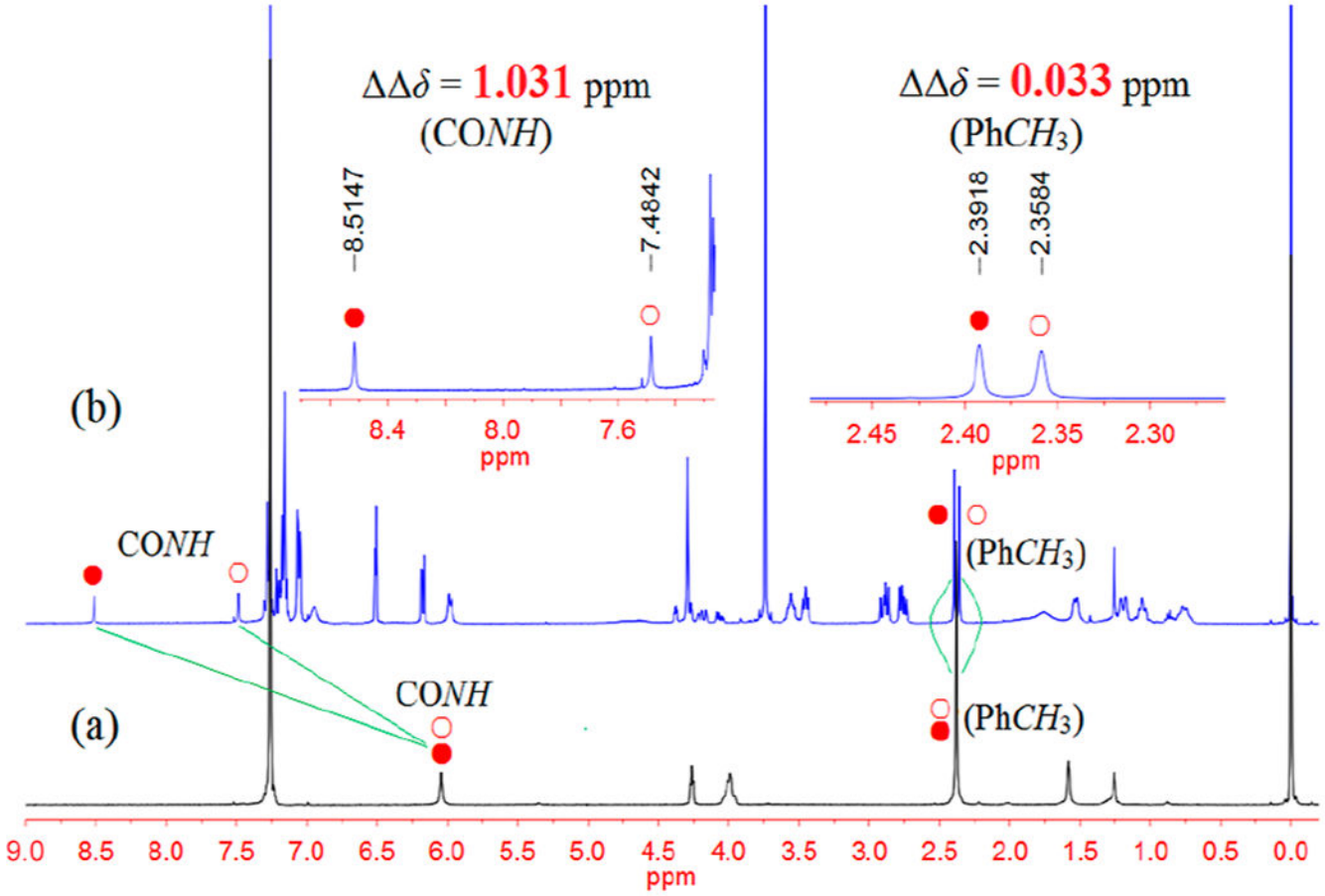

Figure 1.

^{1}H NMR spectra of (±)-G**7** (a) and (±)-G**7** in the presence of TAMCSA **1c** (b) and their expanded spectra in $CDCl_3$ at 25 °C (400 MHz), [(±)-G7] = 10 mM. The marks "red ○"and "red ●" stand for (*S*)-G7 and (*R*)-G7, respectively.

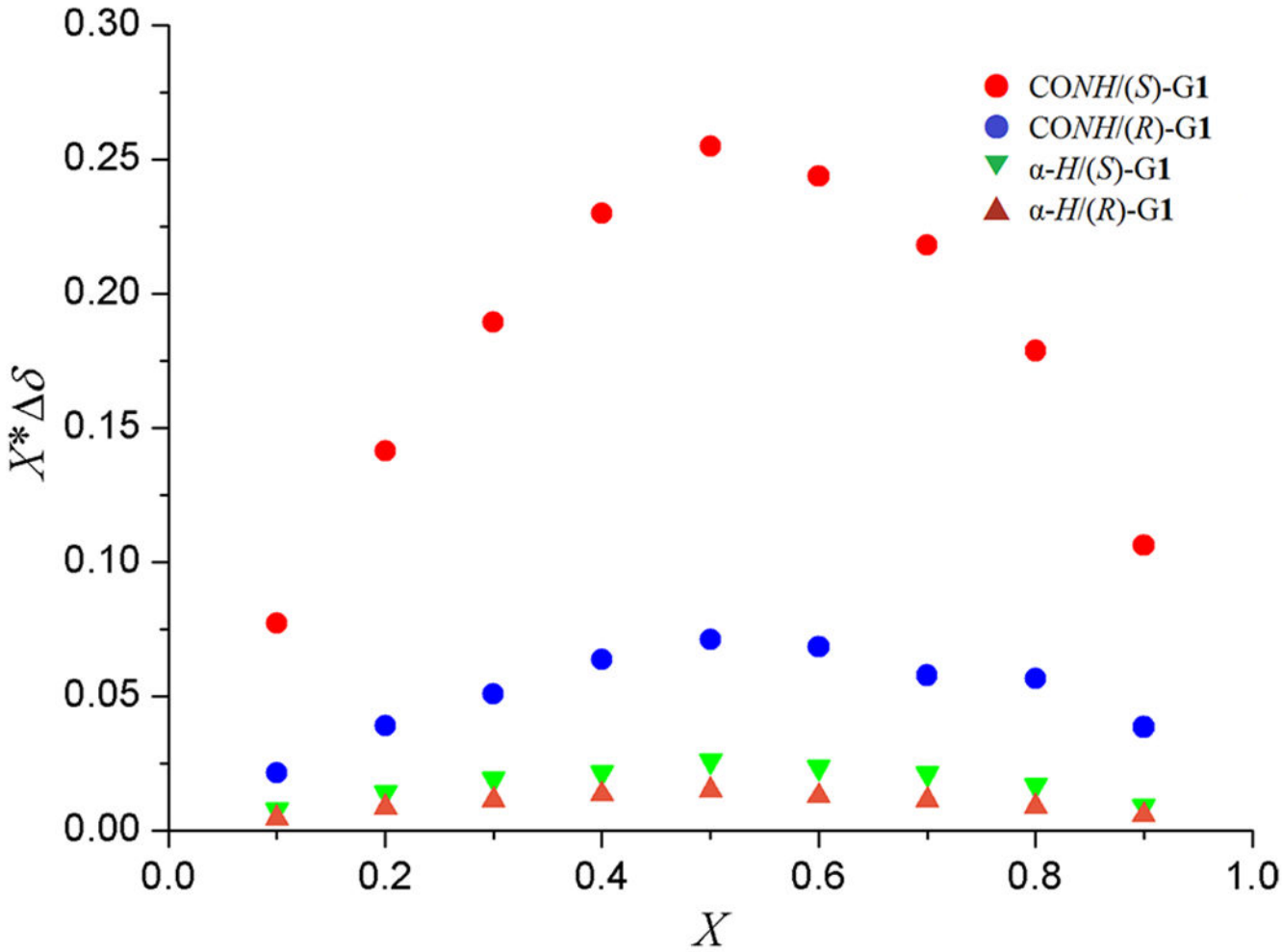

Figure 2.

Job plots for diastereoisomeric complexes of (*S*)-G**1** and (*R*)-G**1** with TAMCSA **1a**. **Δ***δ* stands for the chemical shift change in *NH* (CO*NH*) of (*S*)-G**1** (red ●) and (*R*)-G**1** (blue ●), and Ph*CH* of (*S*)-G**1** (green ▼) and (*R*)-G**1** (red ▲) in the presence of TAMCSA **1a** in $CDCl_3$ at 25 °C (400 MHz). *X* stands for the molar fraction of (±)-G**1**, (*X* = [(±)-G**1**]/[(±)-G**1** + TAMCSA **1a**]).

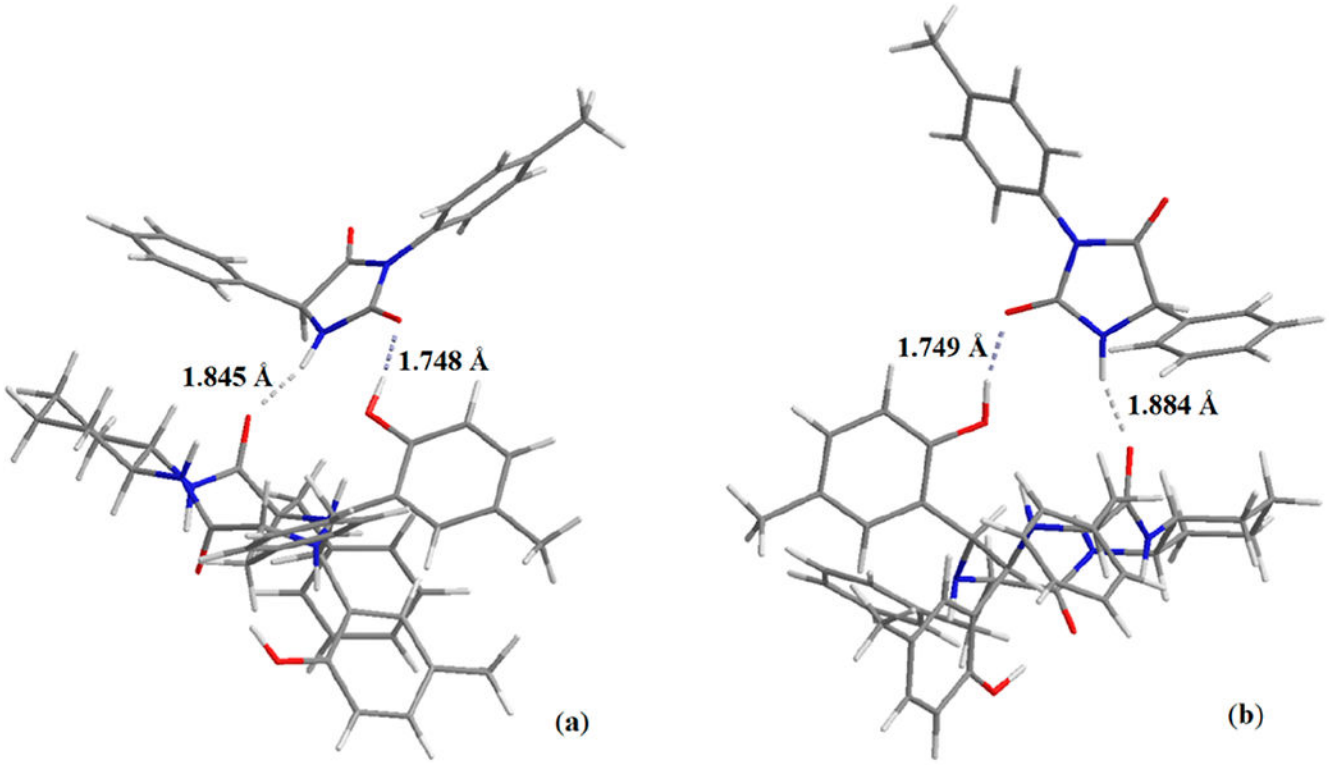

Figure 3.

Proposed DFT models for the hydrogen bonding interactions between (*S*)-G**1** (a) and (*R*)-G**1** (b) with TAMCSA **1a**.

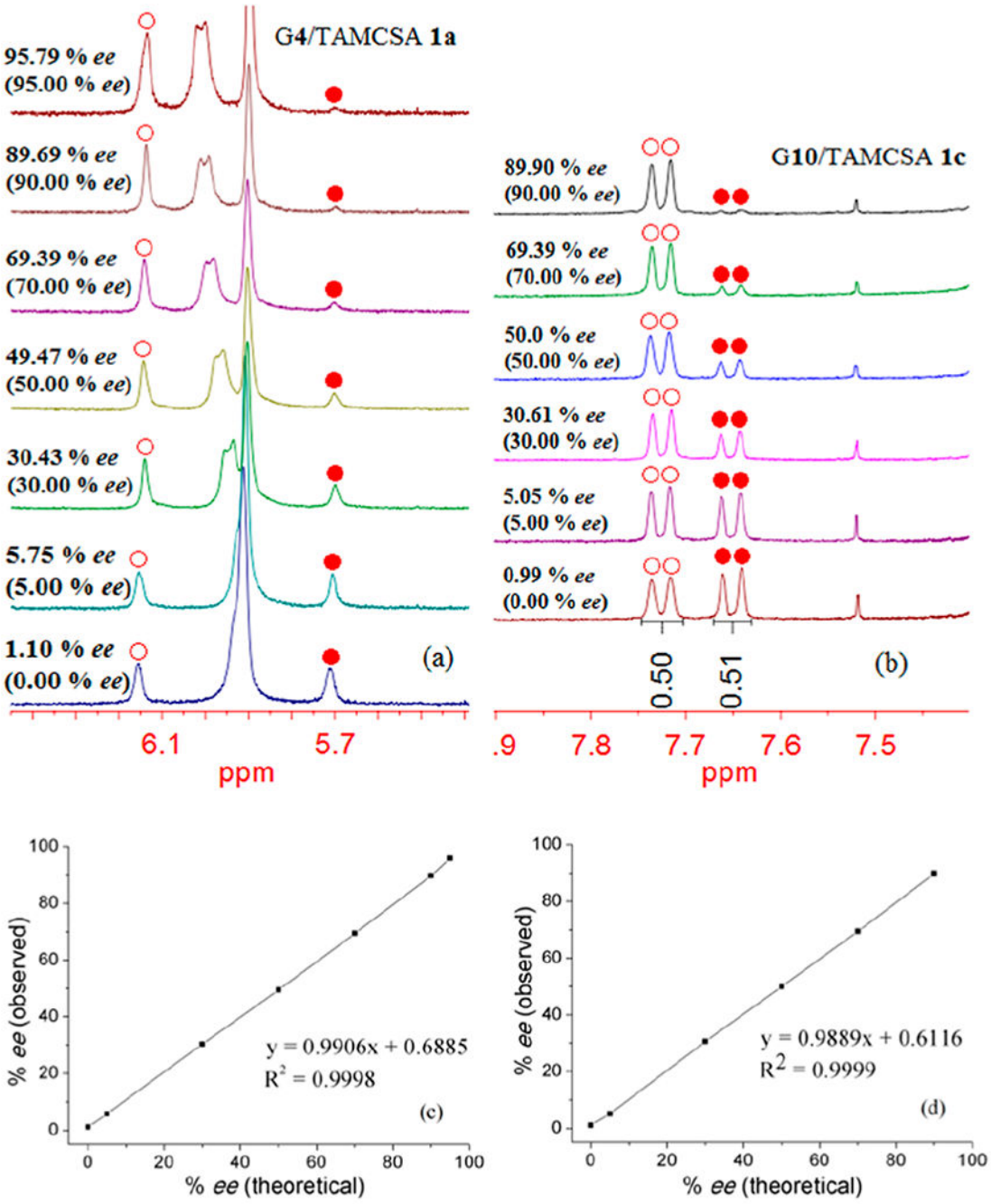

Figure 4.

Determination of ee of G**4** and G**10**, ee (%) = {[(*S*)-G**X** – (*R*)-G**X**]/[(*S*)-G**X** + (*R*)-G**X**]} × 100%, (**X** = **4** and **10**). Overlaid ^{1}H NMR spectra of the *NH* proton (CO*NH*) of (*S*)-G**4** (red ○) and (*R*)-G**4** (red ●) in the presence of TAMCSAs **1a** [5 mM] (a) and (*S*)-G**10** (red ○) and (*R*)-G**10** (red ●) in the presence of TAMCSAs **1c** [7.5 mM] (b) in $CDCl_3$ at 25 °C (400 MHz). Linear correlation between the theoretical (*X*) and observed (*Y*) % values of G**4** with TAMCSA **1a** (c) and G**10** with TAMCSA **1c** (d).

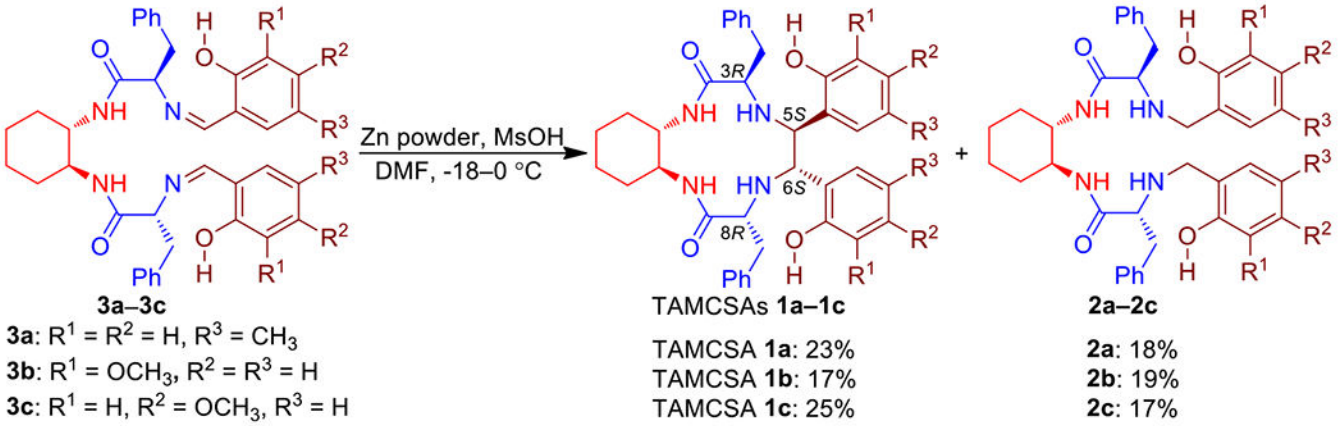

Scheme 1.
Synthesis of TAMCSAs 1a–1c and Chiral Compounds 2a–2c

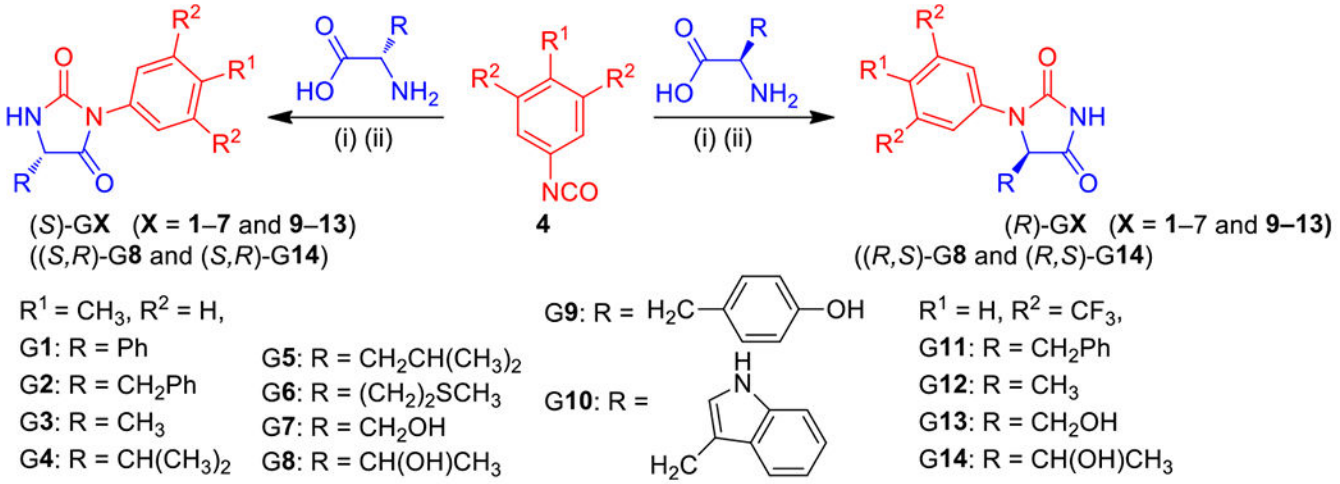

Scheme 2.

Synthesis of Enantiomers of Hydantoin Derivatives 1–14[a]

[a]Conditions: (i) NaOH, CH_3CN, 0 °C and (ii) 1,4-dioxane, rt; HCl, reflux.

Table 1.

Nonequivalent Chemical Shifts ($\Delta\Delta\delta$, ppm) and Partial ^{1}H NMR Spectra of the *NH* Proton (CO*NH*) of (+)-G1–14 in the Presence of TAMCSAs 1a–1c in $CDCl_3$ (400 or 600 MHz) at 25 °C[a]

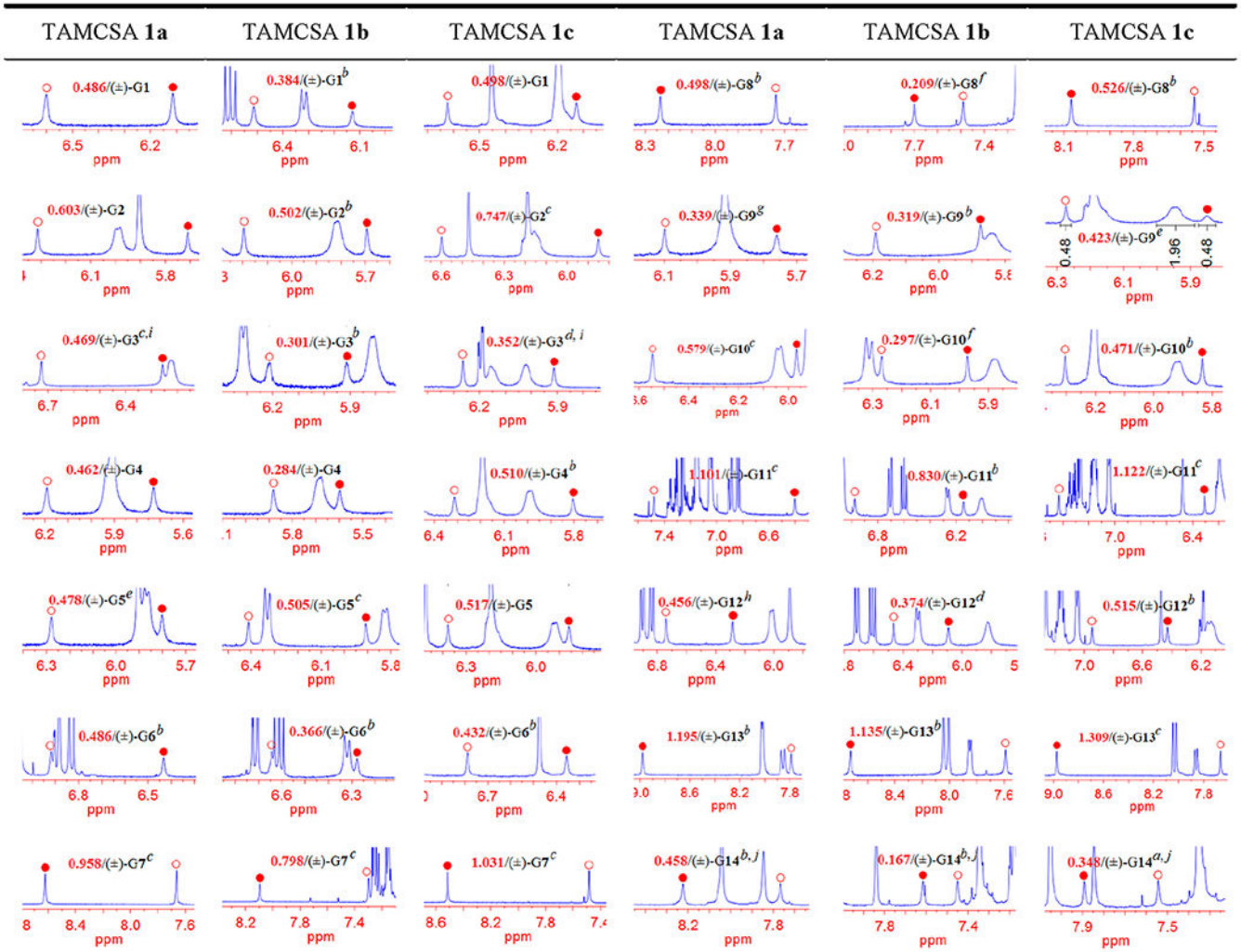

J Org Chem. Author manuscript; available in PMC 2022 September 10.

[a] 5.0 mM.

[b] 7.5 mM.

[c] 10.0 mM.

[d] 6.0 mM.

[e] 4.0 mM.

[f] 12.5 mM.

[g] 2.0 mM.

[h] 3.0 mM.

[i] 600 MHz.

[j] 10% CD_3COCD_3.

Table 2.

Nonequivalent Chemical Shifts ($\Delta\Delta\delta$, ppm) of Other Split Protons of (±)-G1–14 in the Presence of TAMCSAs 1a–1c in $CDCl_3$ (400 or 600 MHz) at 25 °C[a]

guest/TAMCSA	proton	$\Delta\Delta\delta$	guest/TAMCSA	proton	$\Delta\Delta\delta$
(±)-G**1**/**1a**	Ph*CH*	0.030	(±)-G**9**/**1b**[b]	4-PhCH$_2$C*H*	0.024
(±)-G**1**/**1b**[b]	Ph*CH*	0.041	(±)-G**9**/**1c**[e]	Ph*CH*$_3$	0.007
(±)-G**1**/**1c**	Ph*CH*	0.029		4-PhCH$_2$C*H*	0.052
(±)-G**2**/**1a**	Ph*CH*$_2$	0.091	(±)-G**10**/**1a**[c]	*CH*$_2$	0.070
		0.049		*α-H*(trp unit)	0.036
	PhCH$_2$*CH*	0.042		Ar*H*	0.012
(±)-G**2**/**1b**[b]	Ph*CH*$_2$	0.061		Ar*H*	0.119
		0.040		C═CHN*H*	0.031
	PhCH$_2$*CH*	0.031	(±)-G**10**/**1b**[f]	*CH*$_2$	0.051
(±)-G**2**/**1c**[c]	Ph*CH*$_2$	0.111		*α-H*(trp unit)	0.027
		0.054		Ar*H*	0.067
	PhCH$_2$*CH*	0.051		Ar*H*	0.013
(±)-G**3**/**1a**[c,i]	*CH*$_3$	0.049	(±)-G**10**/**1c**[b]	*CH*$_2$	0.045
(±)-G**3**/**1b**[b]	*CH*$_3$	0.020		*α-H*(trp unit)	0.029
(±)-G**3**/**1c**[d,i]	*CH*$_3$	0.029		Ar*H*	0.078
(±)-G**4**/**1a**	(*CH*$_3$)$_2$CHCH	0.014		C═CH*NH*	0.030
		0.042	(±)-G**11**/**1a**[c]	Ph*CH*$_2$	0.153
	(*CH*$_3$)$_2$CH*CH*	0.031			0.100
(±)-G**4**/**1b**	(*CH*$_3$)$_2$CHCH	0.007		PhCH$_2$C*H*	0.086
		0.022		Ar*H*	0.061
	(CH$_3$)$_2$CH*CH*	0.024		Ar*H*	0.014
(±)-G**4**/**1c**[b]	(*CH*$_3$)$_2$CHCH	0.013	(±)-G**11**/**1b**[b]	Ph*CH*$_2$	0.095
		0.044			0.068

J Org Chem. Author manuscript; available in PMC 2022 September 10.

guest/TAMCSA	proton	ΔΔδ	guest/TAMCSA	proton	ΔΔδ
	$(CH_3)_2CHCH$	0.037		$PhCH_2CH$	0.077
(±)-G5/**1a**[e]	CH_3	0.018		ArH	0.058
		0.007		ArH	0.012
	$(CH_3)_2CHCH_2CH$	0.039	(±)-G**11**/**1c**[c]	$PhCH_2$	0.154
(±)-G5/**1b**[c]	CH_3	0.022			0.087
		0.008		$PhCH_2CH$	0.080
	$(CH_3)_2CHCH_2CH$	0.059		ArH	0.061
(±)-G5/**1c**	CH_3	0.020		ArH	0.013
		0.008	(±)-G**12**/**1a**[h]	CH_3	0.034
	$(CH_3)_2CHCH_2CH$	0.045		ArH	0.016
(±)-G6/**1a**[b]	SCH_3	0.030	(±)-G**12**/**1b**[d]	CH_3	0.017
(±)-G6/**1b**[b]	SCH_3	0.021		ArH	0.032
(±)-G6/**1c**[b]	SCH_3	0.025	(±)-G**12**/**1c**[b]	CH_3	0.032
(±)-G7/**1a**[c]	$PhCH_3$	0.038		ArH	0.019
(±)-G7/**1b**[c]	$PhCH_3$	0.023	(±)-G**13**/**1a**[b]	ArH	0.026
(±)-G7/**1c**[c]	$PhCH_3$	0.033		ArH	0.012
(±)-G8/**1a**[b]	CH_3	0.040	(±)-G**13**/**1b**[b]	ArH	0.014
	$PhCH_3$	0.037		ArH	0.040
	$CH_3(OH)CHCH$	0.027	(±)-G**13**/**1c**[c]	ArH	0.022
(±)-G8/**1b**[f]	CH_3	0.050		ArH	0.029
	$PhCH_3$	0.025	(±)-G**14**/**1a**[bj]	CH_3	0.024
	$CH_3(OH)CHCH$	0.024		$CH_3(OH)CHCH$	0.028
(±)-G8/**1c**[b]	CH_3	0.038	(±)-G**14**/**1b**[bj]	CH_3	0.009
	$PhCH_3$	0.035		$CH_3(OH)CHCH$	0.022
	$CH_3(OH)CHCH$	0.027	(±)-G**14**/**1c**[j]	CH_3	0.018

guest/TAMCSA	proton	ΔΔδ	guest/TAMCSA	proton	ΔΔδ
(±)-G**9**/**1a**[g]	PhCH_3	0.005		CH_3(OH)CHCH	0.021
	4-PhCH_2CH	0.030			

[a] 5.0 mM.

[b] 7.5 mM.

[c] 10.0 mM.

[d] 6.0 mM.

[e] 4.0 mM.

[f] 12.5 mM.

[g] 2.0 mM.

[h] 3.0 mM.

[i] 600 MHz.

[j] $CDCl_3$ (10% CD_3COCD_3).

Table 3.

Observed and Calculated Chemical Shift Values (δ, ppm) and Nonequivalent Chemical Shift Values ($\Delta\delta$, ppm) for the *NH* Proton (CONH) of (*S*)-G1 and (*R*)-G1 with TAMCSA 1a

	$\delta_{(S)\text{-G1}}$	$\delta_{(R)\text{-G1}}$	$\Delta\delta^{a}$
obsd values	6.5995	6.1139	0.4856
calcd values	8.6570	8.1340	0.5230

[a] $\Delta\delta = \delta$(*S*)-G**1** - δ(*R*)-G**1**.

Table 4.

Association Constants (K_a, M^{-1}) of (*S*)-G2 and (*R*)-G2 with TAMCSA 1a in $CDCl_3$ (400 MHz)

guest	TAMCSA	K_a (M^{-1})	$-\Delta G°$ (kJ mol^{-1})
(*S*)-G**2**	**1a**	$(3.98 \pm 0.96) \times 10^2$	14.8 ± 4.4
(*R*)-G**2**	**1a**	$(3.83 \pm 1.50) \times 10^2$	14.7 ± 4.3